

American University in Cairo

AUC Knowledge Fountain

Theses and Dissertations

2-1-2015

The expression pattern of circulating miR-590-3p as a promising diagnostic biomarker for early detection of epithelial ovarian cancer

Heba Shawer

Follow this and additional works at: <https://fount.aucegypt.edu/etds>

Recommended Citation

APA Citation

Shawer, H. (2015). *The expression pattern of circulating miR-590-3p as a promising diagnostic biomarker for early detection of epithelial ovarian cancer* [Master's thesis, the American University in Cairo]. AUC Knowledge Fountain.

<https://fount.aucegypt.edu/etds/224>

MLA Citation

Shawer, Heba. *The expression pattern of circulating miR-590-3p as a promising diagnostic biomarker for early detection of epithelial ovarian cancer*. 2015. American University in Cairo, Master's thesis. AUC Knowledge Fountain.

<https://fount.aucegypt.edu/etds/224>

This Thesis is brought to you for free and open access by AUC Knowledge Fountain. It has been accepted for inclusion in Theses and Dissertations by an authorized administrator of AUC Knowledge Fountain. For more information, please contact mark.muehlhaeusler@aucegypt.edu.



THE AMERICAN UNIVERSITY IN CAIRO
الجامعة الأمريكية بالقاهرة

School of Sciences and Engineering

**The expression pattern of circulating miR-590-3p
as a promising diagnostic biomarker for early
detection of epithelial ovarian cancer**

A Thesis Submitted to the
Biotechnology Master's Program
In partial fulfillment of the requirements for the
Degree of Master of Science

By

Heba Shawer

Under the supervision of

Dr. Asma Amleh

Associate Professor

Department of Biology

The American University in Cairo

January 2016

The American University in Cairo

School of Sciences and Engineering (SSE)

The expression pattern of circulating miR-590-3p as a promising diagnostic biomarker for early detection of epithelial ovarian cancer

A Thesis Submitted by

Heba Shower

Submitted to the Biotechnology Master's Program

January 2016

In partial fulfillment of the requirements for the degree of

Master of Science in Biotechnology

Has been approved by

Thesis Committee Supervisor/Chair

Affiliation _____

Thesis Committee Reader/Examiner

Affiliation _____

Thesis Committee Reader/Examiner

Affiliation _____

Thesis Committee Reader/External Examiner

Affiliation _____

Dept. Chair/Director

Date

Dean

Date

DEDICATION

*This thesis work is dedicated
to my beloved Mother, Nagwa El-Hennawi
and my advisor, Dr. Asma Amleh
for their love and support*

ACKNOWLEDGEMENTS

My deepest gratitude is to my advisor, Dr. Asma Amleh for her support, guidance, patience and encouragement. I hope that one day I would become as good to my students as Dr. Asma Amleh has been to me, and I deeply appreciate her belief in me.

I would like to acknowledge Dr. Basel Refky who provided and collected the specimens that were examined in this study. My extended appreciation is to Dr. Khaled Abou Aisha who opened his lab to me to perform the real-time PCR experiments.

I am also thankful to the members of Dr. Amleh's research group. Particularly, Aya El Serw, who performed the semi-quantitative PCR experiments in this work. I am grateful to Aya for her support, care and for bearing with all my ups and downs. I would like to thank Eman El Zeneini and Mai Omar.

I would like to thank my father, Mahmoud Shower and my mother, Nagwa El-Hennawi for supporting me through my graduate studies. I am thankful to my husband and my brothers for their support and encouragement and my son, Adam Amal for inspiring me.

Finally, I would also like to thank the AUC for financially supporting this work.

The expression pattern of miR-590-3p is a promising diagnostic biomarker for early detection of epithelial ovarian cancer

ABSTRACT

Epithelial ovarian cancer (EOC) is the most common type of ovarian tumors. The biomarkers, which are being used for EOC screening, have low sensitivity and specificity leading to late diagnosis and high mortality rate. Thus, identification of effective biomarkers for early diagnosis of ovarian cancer has become a high priority in research. Here we aim to address this problem by studying the expression of a potential molecular marker, miR-590-3p, in EOC. We examined the mRNA steady-state levels of various acknowledged biomarkers including cancer antigen-125 (*CA125*) which is being used for EOC screening, c-reactive protein (*CRP*) which expression was correlated with EOC stage and paired homeobox 2 gene (*PAX2*) whose expression is correlated with the histological grade to characterize the histo-pathological features of the specimens at the molecular level. We examined the expression of miR-590-3p in EOC patients' serum and EOC tissues, using real-time PCR. The levels of circulating miR-590-3p showed to be significantly elevated in 84.6% of the EOC patients' serum, with 76.92% sensitivity and 85.7% specificity at its optimal cutoff value. Tissue miR-590-3p showed to be upregulated in EOC tissues compared to normal ovarian tissues and highly correlated with high-grade poorly differentiated EOC. The adoption of the epithelial-mesenchymal transition biomarkers was enriched in EOC with high miR-590-3p levels. The potential downstream target genes, *SOX2*, *LEF1* and *PAX2*, were predicted using miRanda and Targetscan *in silico* tools and their expression profiles were *in silico* examined using Oncomine data-mining platform and StarBase Pan-cancer analysis. We examined the levels of *SOX2*, *LEF1* and *PAX2* at the RNA and the protein levels via semi-quantitative PCR and western blot, respectively. Among the investigated potential target genes, only *PAX2* showed negative correlation with the levels of miR-590-3p in EOC tissues, suggesting that miR-590-3p could acquire its role in EOC carcinogenesis through regulation of cellular differentiation in EOC.

TABLE OF CONTENTS

DEDICATION.....	iii
ACKNOWLEDGEMENTS.....	iv
ABSTRACT	v
TABLE OF CONTENTS	vi
LIST OF FIGURES	viii
LIST OF TABLES.....	ix
LIST OF ABBREVIATIONS	x
CHAPTER 1: Introduction.....	1
1.1 Ovarian Cancer	1
1.2 Epithelial ovarian cancer	1
1.3 Biomarkers and screening methods for ovarian cancer.....	2
1.3.1. Current biomarkers.....	2
1.3.2 MicroRNA potential biomarker	3
1.3.2.a MiRNA biogenesis	3
1.3.2.b MiRNA gene expression regulation.....	5
1.3.3 Circulating miRNAs are emerging cancer biomarkers.....	5
1.3.4 Circulating miRNAs in ovarian cancer.....	7
1.4 Scope of the study and Study objectives.....	10
CHAPTER 2: Materials and Methods	13
2.1 Study participants and sampling.....	13
2.2 Total RNA extraction from serum and tissue samples.....	14
2.3 Semi-quantitative reverse transcription-polymerase chain reaction (RT-PCR)	15
2.4 Quantitative real-time RT-PCR.....	16
2.5 Western blot analysis.....	17
2.6 Target gene prediction and miRNA functional analysis.....	18
2.7 Statistical analysis	19
CHAPTER 3: Results.....	20
3.1 Clinico-pathologic Characteristics.....	20
3.2 Histo-pathological characterization at the molecular level.....	23
3.3 Upregulation of serum miR-590-3p in EOC patients	26
3.4 Serum miR-590-3p level is a promising diagnostic marker for epithelial ovarian cancer.....	29
3.5 Upregulation of miR-590-3p in EOC tissues	30
3.6 The correlation between miR-590-3p levels and epithelial–mesenchymal transition (EMT) in EOC.....	32
3.7 Bioinformatics analysis of miR-590-3p potential target genes.....	33

3.8 <i>The expression of the predicted target genes and its correlation with miR-590-3p in EOC tissues.....</i>	40
3.9 <i>MiR-590-3p expression profiles in different cancer types</i>	43
CHAPTER 4: Discussion, Conclusions and Future directions	45
References.....	51
Appendix A: Real-time PCR Amplification Plot	59
Appendix B: Quantitative real-time RT-PCR Comparative C_T Analysis Serum Samples	60
Appendix C: Quantitative real-Time RT-PCR Comparative C_T Analysis Tissue samples...63	63
Appendix D: IRB Approval	67
Appendix E: Patient’s Consent Forms	68
Appendix F: Copyrights Form	72

LIST OF FIGURES

Figure 1: MicroRNA biogenesis and post-transcriptional gene expression regulation.	4
Figure 2: Circulating miRNA packaging and release into blood stream.	6
Figure 3: Schematic flow chart of the Taq-man quantitative real-time PCR experiments.	12
Figure 4: Histological grade of EOC samples.	22
Figure 5: RT-PCR analysis of tissue <i>CA125/Mucin16</i> shows elevated levels in EOC relative to control tissues (P=0.0001).	24
Figure 6: Higher levels of CRP were associated with advanced stages of EOC.	25
Figure 7: The level of <i>PAX2</i> mRNA in EOC samples is a marker for EOC histological grade.	26
Figure 8: miR-590-3p is significantly elevated in EOC patients' serum.	27
Figure 9: The correlation between serum miR-590-3p levels and EOC clinicopathological features.	28
Figure 10: Receiver-operator characteristics (ROC) curve analyses of circulating miR-590-3p for EOC patients versus healthy controls.	29
Figure 11: MiR-590-3p expression in EOC tissues.	31
Figure 12: The mRNA steady state levels of EMT markers in EOC and control ovarian tissues.	33
Figure 13: Downregulation of <i>SOX2</i> in ovarian cancer relative to normal ovarian tissues.	36
Figure 14: Computational analysis depicts <i>LEF1</i> as a potential target gene for miR-590-3p.	37
Figure 15: <i>In silico</i> analysis of <i>PAX2</i> as a potential downstream target of miR-590-3p.	38
Figure 16: <i>SOX2</i> expression is not significantly correlated to miR-590-3p levels in EOC tissues.	41
Figure 17: The correlation between <i>LEF1</i> expression and miR-590-3p in EOC.	42
Figure 18: The correlation between the expression of <i>PAX2</i> and miR-590-3p.	43
Figure 19: Expression profiles of miR-590-3p among different cancer types.	44

LIST OF TABLES

Table 1: Summary of the dysregulated extracellular miRNAs in ovarian cancer.	8
Table 2: Summary of the clinical characteristics of patients in the study.....	13
Table 3: Primers used for semi-quantitative PCR.....	15
Table 4: Taq-Man MicroRNA Assays.....	17
Table 5: Clinical characteristics of EOC patients in the study.	20
Table 6: The levels of tissue <i>CRP</i> in different stages of EOC.....	21
Table 7: The levels of tissue <i>PAX2</i> in different histological grades.	22
Table 8: The alignment features of the putative miR-590-3p targets.	39

LIST OF ABBREVIATIONS

Ago2	Argonaute 2 protein
AIMP3	Aminoacyl- tRNA synthetase-Interacting Multifunctional Protein-3
ANOVA	Analysis of Variance
AUC	Area Under the receiver-operating characteristic Curve
Bta	Bos Taurus
CA125	Cancer antigen 125
cDNA	Complementary DNA
Cfa	Canis familiaris
CI	Confidence Interval
Cpo	Cavia porcellus
CRP	C-Reactive Protein
Dno	Dasypus novemcinctus
dsRBD	Double-stranded RNA-binding protein
EIF4H	Eukaryotic Initiation Factor 4H gene
EMT	Epithelial–Mesenchymal Transition
EOC	Epithelial Ovarian Cancer
Fca	Felis catus
FIGO	International federation of Gynecology and Obstetrics
GAPDH	Glyceraldehyde-3-Phosphate Dehydrogenase
GBM	Glioblastoma
HCC	HepatoCellular Carcinoma
HE4	Human Epididymal protein4

hnRNPs	Heterogeneous nuclear ribo-nucleoproteins
HNSC	Head-Neck Squamous Cell Carcinoma
Hsa	Homo sapiens
Hsa-miR-590-3p	Homo sapiens microRNA-590-3p
IRB	Institutional Review Board
LEF1	Lymphoid Enhancer-binding Factor1
Mdo	Monodelphis domestica
mESCs	Mouse Embryonic Stem Cells
mins	Minutes
MiRNA	MicroRNA
Mml	Macaca mulatta
Mmu	Mus musculus
mRNA	Messenger RNA
MV	Microvesicles
MVB	Multivascular bodies
Ng	Nano gram
Oga	Otolemur garnetti
ORF	Open Reading Frame
OVCA	Ovarian Cancer
OVCA-432	Ovarian serous adenocarcinoma cell line
OVCAR-3	High-grade ovarian serous adenocarcinoma cell line
P-value	Probability value
PAX2	Paired homeobox 2 gene
PBS	Phosphate-buffered saline

PCR	Polymerase chain reaction
Pre-miRNA	miRNA precursor
Pri-miRNA	Primary miRNA transcript
Ptr	Pan troglodytes
QRT-PCR	Quantitative Reverse transcription-polymerase chain reaction
RISC	RNA-induced silencing complex
RNA	Ribonucleic acid
Rno	Rattus norvegicus
ROC	Receiver Operating Characteristic
rpm	Revolutions per minute
RT-PCR	Reverse transcription-polymerase chain reaction
SDS	Sodium Dodecyl Sulfate
secs	Seconds
snRNA	Small nuclear RNA
SOX2	Sex determining region-Y-related high mobility group box 2
TCGA	The Cancer Genome Atlas
THCA	Thyroid carcinoma
Tov21g	Malignant ovarian clear cell adenocarcinoma cell line
TRBP	Transactivation-responsive RNA-binding protein
μl	Micro-liters
3'UTR	3' Un-Translated Region

CHAPTER 1

Introduction

1.1 Ovarian Cancer

Ovarian cancer (OVCA) is the most lethal cancer in the female reproductive system (Howlader N, 2015). In developing countries, ovarian cancer represents 18.8% of all types of gynecological cancers (Jemal et al., 2011). The worldwide ovarian cancer deaths in 2008, was estimated to be 140,200 deaths out of 225,500 ovarian cancer cases, with 54% of the worldwide ovarian cancer deaths and 55% of the worldwide ovarian cancer cases found in the developing countries (Jemal et al., 2011). Moreover, the five-year survival among ovarian cancer cases is less than 50% (Sankaranarayanan & Ferlay). This high mortality is mainly due to the diagnosis of ovarian cancer at advanced stages. About 70% of the patients are diagnosed at late stages and that is mainly due to the absence of effective screening methods (Gang et al., 2012). Thus, OVCA is called the “silent killer”, as the symptoms are not very beneficial for diagnosis because they are similar to that of gastrointestinal and gynecological disorders (Gang et al., 2012). The most common type of ovarian cancer is the epithelial ovarian cancer (EOC) that accounts for about 90% of the ovarian cancer cases. EOC is a highly heterogeneous disease and its etiology is still not fully understood.

1.2 Epithelial ovarian cancer

The origin of EOC and its etiology are not clear and are strongly debated. Early studies used to believe that EOC was derived from the mesothelium, which is the ovarian surface epithelium, as reviewed by (Dubeau, 2008). Nonetheless, recent studies proposed that EOC was originated from müllerian-type tissues (Bast et al., 2009). EOC is classified into various histological subtypes, which are serous, mucinous, endometrioid, transitional (Brenner), and clear cell, as reviewed by (V. W. Chen et al., 2003). The morphological features of the serous type are similar to that of the fallopian tube epithelium. Mucinous and endometrioid types have similar morphology to that of the endocervical epithelium and endometrium, respectively. The cervix, endometrium and fallopian tubes are originated from müllerian-type tissue. Therefore, EOC shows müllerian phenotype, supporting that it could be originated from müllerian-derived tissues (Bast et al., 2009).

There are three histological grades of EOC based on the degree of tumor cell differentiation. Grade-I is characterized by its well-differentiated cellular appearance. Grade-II tumor is characterized by having moderately differentiated tumor cells and grade-III tumors are made up of poorly differentiated cells. EOC can be classified into four stages depending on the degree of the tumor spread. The stage of the tumor can be determined by radiologic evaluation and surgically (Heintz et al., 2006). The EOC staging is classified based on the International Federation of Gynecology and Obstetrics (FIGO) criteria (Heintz et al., 2006). In stage-I tumors, the tumor is limited to the ovaries, could be one (IA) or both of the ovaries (IB). Stage-II tumors are more spread involving both of the ovaries and uterus (IIA) and could have extension to the pelvic area (IIB/IIC). Stage-III tumors involving the ovaries, with confined intra-peritoneal metastases outside the pelvis (IIIA/IIIB) and/or extension to the peritoneal lymph nodes (IIIC). Finally, stage-IV tumors spread beyond the ovaries to reach distant organs as the lungs (Heintz et al., 2006).

1.3 Biomarkers and screening methods for ovarian cancer

1.3.1. Current biomarkers

Cancer antigen (CA) 125 is the most popular biomarker for ovarian cancer diagnosis. CA125 is a glycoprotein that was found to be elevated in the blood of about 80% of EOC patients and in only 50% of patients at early stages (Havrilesky et al., 2008; Rosen et al., 2005). CA125 gives indication to ovarian cancer progression and response to chemotherapy. Also, its levels were found to be elevated in benign cases as in pregnancy or fibroids. Therefore, CA125 blood test is being used for ovarian cancer diagnosis along with vaginal examination and along with other biomarkers, as the Human Epididymal Protein 4 (HE4), in order to increase the sensitivity and specificity of the test (Gadducci et al., 2009; Gang et al., 2012; Rosen et al., 2005).

The Human Epididymal Protein 4 (HE4) is a glycoprotein normally expressed in the female reproductive system and is elevated in ovarian cancer cases (Ławicki et al., 2013). The specificity and sensitivity of HE4 as a biomarker for ovarian cancer is enhanced, when used in conjunction with CA125 blood test (Havrilesky et al., 2008; Ławicki et al., 2013). The use of HE4 along with CA125 can differentiate between benign conditions

and ovarian cancer, which can't be distinguished by CA125 alone (Gang et al., 2012). However, their low sensitivity and low specificity necessitate the development of a new efficient biomarker.

1.3.2 MicroRNA potential biomarker

MicroRNAs (miRNAs) expression and their use as biomarkers for EOC is a promising field of study. Circulating miRNAs are remarkably stable and easily detected. The dysregulation of extracellular miRNAs was observed in various diseases, including cancer.

1.3.2.a MiRNA biogenesis

MiRNAs are mainly transcribed by RNA Polymerase II, producing primary miRNA transcript (pri-miRNA) (Y. Lee et al., 2004). RNA Polymerase III transcribes certain miRNA genes, located within Alu- repetitive elements in chromosome 19 (Borchert et al., 2006). Several miRNA genes are located close to each other and are transcribed as long polycistronic primary miRNA (pri-miRNA) transcripts (Y. Lee et al., 2004). Pri-miRNAs are stem-loop transcripts with length from hundreds to thousand of nucleotides with poly-adenylated 3' end, and 5' cap structures (Y. Lee et al., 2002). In the nucleus, the pri-miRNA is processed into hairpin-shaped intermediate 60 to 70 nucleotides in length called miRNA precursor (pre-miRNA) by microprocessor multi-protein complex (Gregory et al., 2004). The microprocessor complex consists of Drosha nuclear RNase III enzyme, a double-stranded RNA-binding protein (dsRBD) called DGCR8/Pasha and co-factors, such as RNA helicases and heterogenous nuclear ribo-nucleoproteins (hnRNPs). DGCR8/Pasha protein binds to pri-mRNA at the single stranded RNA- double stranded RNA junction in order to direct the Drosha RNase III enzyme to cut the strands of the stem at the base of the stem loop. Drosha cleavage generates pre-miRNA with 5' mono-phosphate and 2 nucleotides 3' overhang which is characteristic for RNase III cleavage (Y. Lee et al., 2002).

The pre-miRNA is then transported in the presence of GTP from the nucleus to the cytoplasm by exportin-5 that recognizes the 3' overhang (Gregory et al., 2004). The pre-miRNA undergoes further processing in the cytoplasm by Dicer RNase III enzyme and RNA-induced silencing complex (RISC) (Figure 2). RISC complex encompasses the

Argonaute 2 (Ago2) protein and the transactivation-responsive RNA-binding protein (TRBP). The Ago2 binds to the pre-miRNA and cleaves its 3' end through exonucleolytic trimming and then Dicer induce further cleavage of the Ago2-cleaved pre-miRNA to generate mature miRNA duplex (Hutvagner et al., 2001). The miRNA mature strand is loaded into the RISC complex and guides the miRNA-RISC complex to the complementary sequence in the target mRNA. It mainly represses gene expression by inducing mRNA degradation through the endonuclease activity of the Ago protein that can cleave miRNA-mRNA double stranded complex (Hutvagner & Zamore, 2002) or through mRNA destabilization via inducing mRNA deadenylation (Behm-Ansmant et al., 2006; Wu et al., 2006) or can inhibit the translation of the target mRNA (Nottrott et al., 2006; Petersen et al., 2006). MiRNA biogenesis encompasses various complexes that cleave, export and generate the mature miRNA. They themselves are regulated by diverse mechanisms to ensure the proper miRNA regulation. Each step in the miRNA biogenesis, from transcription till binding to the target mRNA, plays a regulatory function that controls the production level of miRNAs and regulates the miRNA-mediated gene expression regulation.

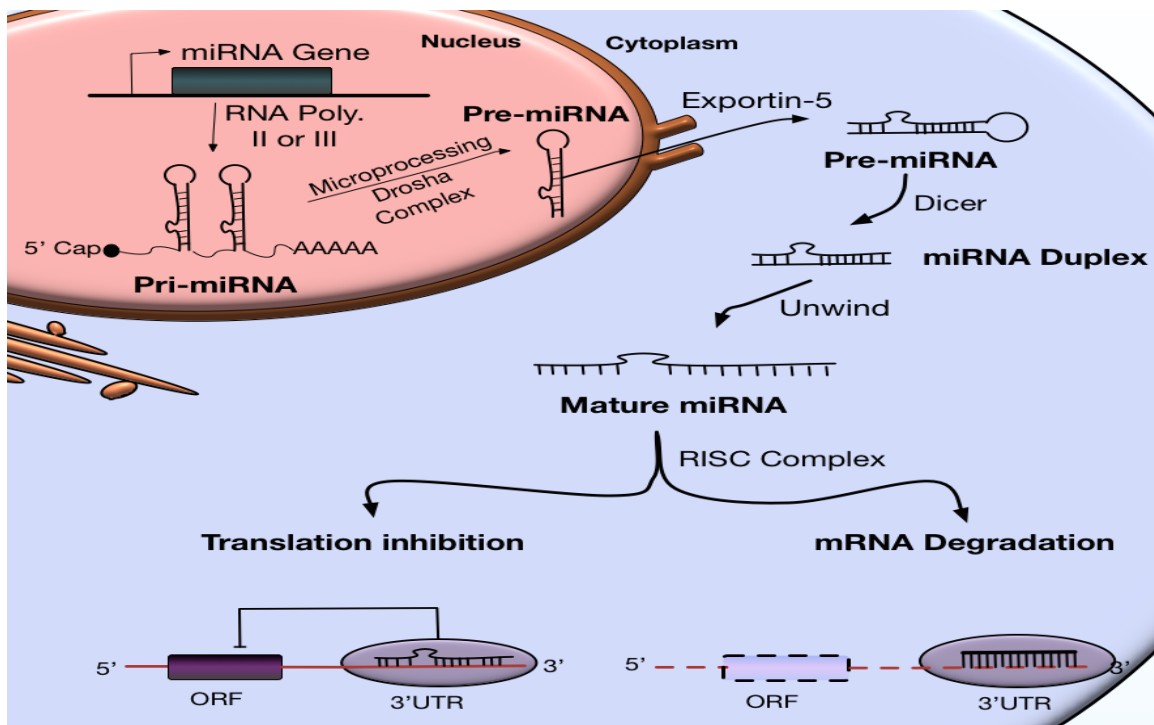


Figure 1: MicroRNA biogenesis and post-transcriptional gene expression regulation. In the nucleus, miRNAs are transcribed by RNA polymerase II/III and producing primary

miRNA transcript (pri-miRNA), which is cleaved by Drosha-DGCR8 endonuclease complex to produce miRNA precursors (pre-miRNA). The pre-miRNA is exported to the cytoplasm through exportin-5 and then undergoes further processing in the cytoplasm by ribonuclease Dicer generating miRNA duplex. The duplex unwinds producing a single stranded mature miRNA that is incorporated into RISC complex and serve as a guide for mRNA targeting resulting mainly in translation inhibition or mRNA degradation. The figure was generated using OmniGraffle 6.4.1.

1.3.2.b MiRNA gene expression regulation

MiRNAs, which are small noncoding single stranded RNA of around 20 to 25 nucleotides in length, regulate the expression of more than 30% of the human protein-coding genes (Xiaohui et al., 2005). They regulate various biological processes including cell proliferation, tissue differentiation and developmental timing. The abnormal expression of miRNAs is involved in various types of cancers and can be used in diagnostic and prognostic analyses (Thomson et al., 2006). Alterations in miRNA expression are associated with abnormal cell development in cancer. MiRNAs may act as oncogene or tumor suppressor depending on their target gene. MiRNAs mainly act by imperfect base pairing with the target mRNA. It mainly represses gene expression by destabilization of the transcript or by translational inhibition (Figure 1). A single miRNA targets more than one mRNA and the disruption in the miRNA mediated gene regulation affects tissue differentiation and is associated with various diseases, including cancer.

1.3.3 Circulating miRNAs are emerging cancer biomarkers

Secretory miRNAs were detected in various body fluids, including plasma, serum, urine, breast milk and saliva (Hunter et al., 2008; Kosaka et al., 2010). Unexpectedly, miRNAs in body fluids showed to be remarkably stable, even under harsh conditions as in repeated freezing and thawing, prolonged storage at room temperature, as well as being resistant to RNase activity and resistant to extreme pH levels (Mitchell et al., 2008). This high stability mainly accounts to miRNA inclusion in microvesicles, exosomes, lipoproteins, RNA-binding protein complexes or apoptotic bodies (El-Hefnawy et al., 2004; Hunter et al., 2008) (figure-2). Exosomes are double lipid layer 50-90 nm vesicles that are released from the donor cells by fusion of multivesicular bodies (MVB) with the plasma membrane (Février & Raposo, 2004). Microvesicles (MV) are larger vesicles (0.1-1 μm) released through outward shedding of the plasma membrane (Hunter et al., 2008). Also, miRNA are included in apoptotic bodies (0.5-2 μm), which are shed from cells during apoptosis

(Zernecke et al., 2009). Valadi and colleagues showed that exosomal miRNAs are secreted from donor cells to the blood stream and are uptaken by endocytosis to regulate gene expression in the recipient cell as a form of cell-cell communication (Valadi et al., 2007).

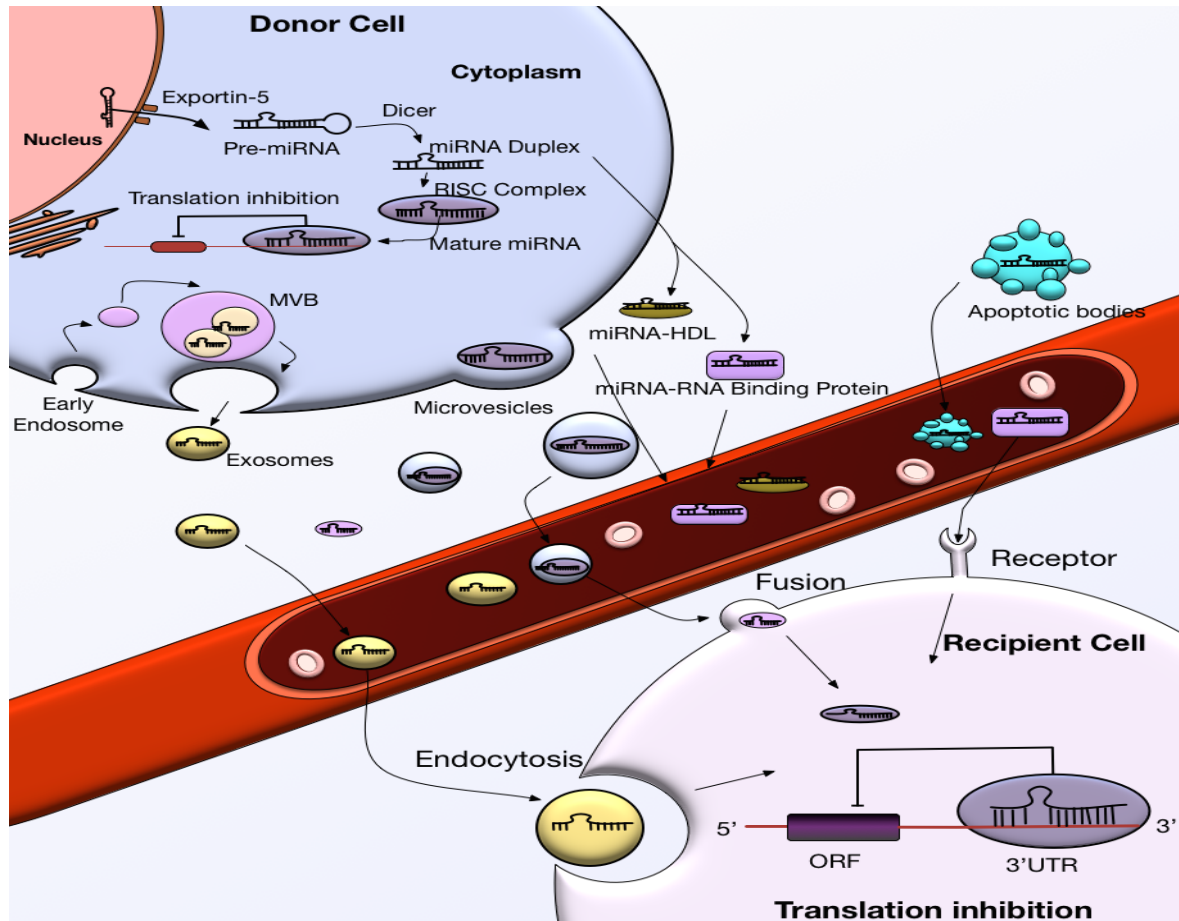


Figure 2: Circulating miRNA packaging and release into blood stream. Mature miRNAs are released from the cell through various mechanisms, including sorting into MVB that are discharged by exosomes, outward shedding of microvesicles that encompass miRNA, miRNA may also be released by incorporation into RNA-binding proteins or high-density lipoproteins (HDL). Also, apoptotic bodies could convey miRNAs into the blood stream. Circulating miRNAs also serve in cell-to-cell communication. The figure was generated using OmniGraffle 6.4.1.

The levels of circulating miRNAs are highly affected by various diseases including cancer. Therefore, they are considered as minimally invasive potential biomarkers for the diagnosis and prognosis of cancer. Selected cellular miRNAs showed be designated for extracellular release via exosomes. Where, Pigati and colleagues reported that only 66% of the cellular miRNA are released to the extracellular space at levels corresponding to

the cellular miRNA levels (Pigati et al., 2010) and 21% of the cellular miRNAs were found at excessively higher levels in the cell-derived exosomes than that of the mother cells. The remaining 13% of the miRNAs were selectively kept inside the cell without extracellular release. Moreover, the selection of the secreted miRNAs was significantly affected by malignancy (Pigati et al., 2010). The selective miRNA release could also reflect the stage of cancer, the response to treatment, metastasis and cancer prognosis. This infers that the cell employs certain mechanisms to designate certain miRNAs to be released via the vesicles to the body fluids. These mechanisms of secretory miRNAs selection and the role of these circulatory miRNAs are still not fully understood.

1.3.4 Circulating miRNAs in ovarian cancer

Taylor and Gercel-Taylor showed that the levels of circulating tumor-derived exosomes were significantly elevated in ovarian cancer patients relative to patients with benign ovarian tumor and healthy females. (Taylor & Gercel-Taylor, 2008). Several miRNAs were identified to be dysregulated in the serum of ovarian cancer patients. Resnick and colleagues identified five miRNAs, miR-21, miR-92, miR-93, miR-126 and miR-29a, elevated in the serum of ovarian cancer patients and another three downregulated miRNAs, miR-155, miR-127 and miR-99b (Resnick et al., 2009). Serum miR-145 was described to be downregulated in ovarian cancer patients compared to healthy controls (Table 1) (Liang et al., 2015). In another study, the combination of the elevated plasma miR-205 levels and reduced plasma let-7f levels in ovarian cancer patients were proposed as a potential diagnostic tool (Table 1) (Kan et al., 2012; Zheng et al., 2013). Serum miR-200 family were found to be elevated in other cancer types including colorectal cancer (Toiyama et al., 2014), gastric cancer (Valladares-Ayerbes et al., 2012), breast cancer (Antolin et al., 2015) and hepatocellular carcinoma (Dhayat et al., 2015).

Table 1: Summary of the dysregulated extracellular miRNAs in ovarian cancer.

Differentially expressed miRNAs	The body fluid	Approach	AUC*	Sensitivity	Specificity	Population	Reference
Combination of miR-205 (Up) + Let-7f (Down)	Plasma	TaqMan low-density array Real-time- PCR	0.831	62.4%	92.9%	EOC (n=260), Healthy controls (n=200)	(Zheng et al., 2013)
miR-200c (Up) miR-141 (Up)	Serum	Real-time PCR	0.79 0.75	72% 69%	70% 72%	EOC (n=74), Healthy controls (n=50)	(Gao & Wu, 2015)
miR-21, miR-92, miR-93, miR-126 and miR-29a (Up) miR-155, miR-127 and miR-99b (Down)	Serum	TaqMan Array Human MicroRNA panel Real-time PCR	n/a**	n/a	n/a	EOC (n=28), Healthy controls (n= 15)	(Resnick et al., 2009)
miR-145 (Down)	Serum	Real-time PCR	0.82	n/a	n/a	Malignant OVCA (n=84), Healthy control (n=135)	(Liang et al., 2015)
miR-106b, miR-126, miR-150, miR-17, miR-20a, and miR-92a (Up)	Plasma	Taqman Open Array MicroRNA pools	<0.8 >0.8	n/a	n/a	Serous EOC (n=42), Healthy controls (n=23)	(Shapira et al., 2014)
miR-92 (Up)	Serum	Real-time PCR	0.8	80.7%	75%	EOC (n=50), Healthy controls (n=50)	(Guo et al., 2013)

miR-30a-5p (Up)	Urine	miRNA microarray Real-time PCR	0.862	n/a	n/a	Serous EOC (n=39), Healthy controls (n=30)	(Zhou, 2015)
miR-221 (Up)	Serum	Real-time PCR	n/a	n/a	n/a	EOC (n=96), Healthy controls (n=35)	(Hong et al., 2013)
miR-21 (Up)	Serum	Real-time PCR	n/a	n/a	n/a	EOC (n=94), Healthy controls (n=40)	(Yun-Zhao Xu1, 2013)
U2-1 snRNA (Up)	Serum	Microarray Real-time PCR	n/a	n/a	n/a	OVCA (n=119), Healthy controls (n=35)	(Kuhlmann et al., 2014)

*AUC: area under the receiver operating characteristic curve.

** n/a: not available

1.4 Scope of the study and Study objectives

Various miRNAs were reported to have a role in EOC development. However, the role of miR-590-3p in EOC was not studied before. Here, we employed various bioinformatics analysis to identify the potential role of miR-590-3p in EOC development. Our initial analysis suggested that miR-590-3p could have a role in tumor initiation, through regulating vital cellular pathways including cell differentiation processes. Additionally, the diagnostic potential of the circulating miR-590-3p was never investigated in cancer patients, despite being listed among the twenty most abundant miRNAs in most of the body fluids (Weber et al., 2010). Our aim is to study the levels of circulating miR-590-3p in the serum as a potential minimally invasive biomarker for the diagnosis of EOC, as well as investigating its potential role in EOC carcinogenesis. The human miR-590-3p (hsa-miR-590-3p) is an intragenic intronic miRNA, 21 nucleotides in length, located within intron number 5 of the eukaryotic initiation factor 4H (EIF4H) gene and is located at chromosome 7: 73605528-73605624 [+]. The basic expression of miR-590-3p was detected at its highest levels in the heart, followed by the testes and the kidneys; nonetheless minimal levels were detected in the brain and the cerebellum.

Previous studies described the role of miR-590-3p in stem cells. In normal human mesenchymal stem cells, miR-590-3p ectopic expression increased cell proliferation and clonogenicity, as well as reducing cellular senescence via the direct downregulation of aminoacyl- tRNAsynthetase-interacting multifunctional protein-3 (AIMP3/p18), which is also a tumor suppressor gene (S. Lee et al., 2014). Also, miR-590 plays a role in DNA repair of the double strand breaks and the single strand breaks that could occur during the rapid proliferation of the mouse embryonic stem cells (mESCs), without affecting its stemness features (Liu et al., 2014). In adult cardiomyocytes that have limited low proliferation ability, miR-590-3p induced-expression resulted in cell cycle re-entry and promoted adult cardiomyocytes proliferation (Eulalio et al., 2012).

In previous studies, altered expression of miR-590-3p was detected in bladder cancer, glioblastoma and hepatocellular carcinoma. Nevertheless, the published studies about miR-590-3p in cancer reached opposing or inconsistent conclusions. In bladder cancer, miR-590-3p was downregulated relative to the normal and adjacent tumor tissues and

induced-overexpression of miR-590-3p in bladder cancer cell lines inhibited cell proliferation, migration and colony formation (Mo et al., 2013). On the other hand, miR-590-3p was significantly upregulated in in hepatocellular carcinoma (HCC) tissues and cell lines, and the ectopic expression of miR-590-3p promoted HCC cell proliferation (H. Yang et al., 2013). Yan and colleagues examined miRNA expression in 116 samples of low-grade gliomas, anaplastic gliomas and secondary glioblastomas using microarray and quantitative real-time PCR analysis and they reported that miR-590-3p was significantly upregulated in anaplastic gliomas and secondary glioblastomas relative to low-grade gliomas, in both the microarray screening cohort and the qPCR validation cohort (Yan et al., 2014). However, in a recent study that was also about glioma, Pang and colleagues reported that miR-590-3p was downregulated in glioma tissues and cell lines compared to non-neoplastic brain tissues and primary normal human astrocytes (Pang et al., 2015). The differing data about the expression pattern of miR-590-3p in cancer suggests that miR-590-3p could play its role in a certain stage of tumor development, thus further studies need to be conducted to clarify the role of miR-590-3p in carcinogenesis.

The specific objectives of the study are:

1. Studying the diagnostic ability of the circulating miR-590-3p by examining its levels in EOC patients' serum, as well as the levels of miR-590-3p in EOC tissues relative to healthy controls. The experimental design of the real-time PCR experiments is illustrated in Figure 3.
2. Studying the potential association of miR-590-3p levels with epithelial-mesenchymal transition.
3. Investigating the potential role of miR-590-3p in EOC through studying its potential downstream targets in EOC.
4. Studying the expression profiles of miR-590-3p in different cancer types, through utilizing the expression data available at The Cancer Genome Atlas (TCGA) Data Portal.

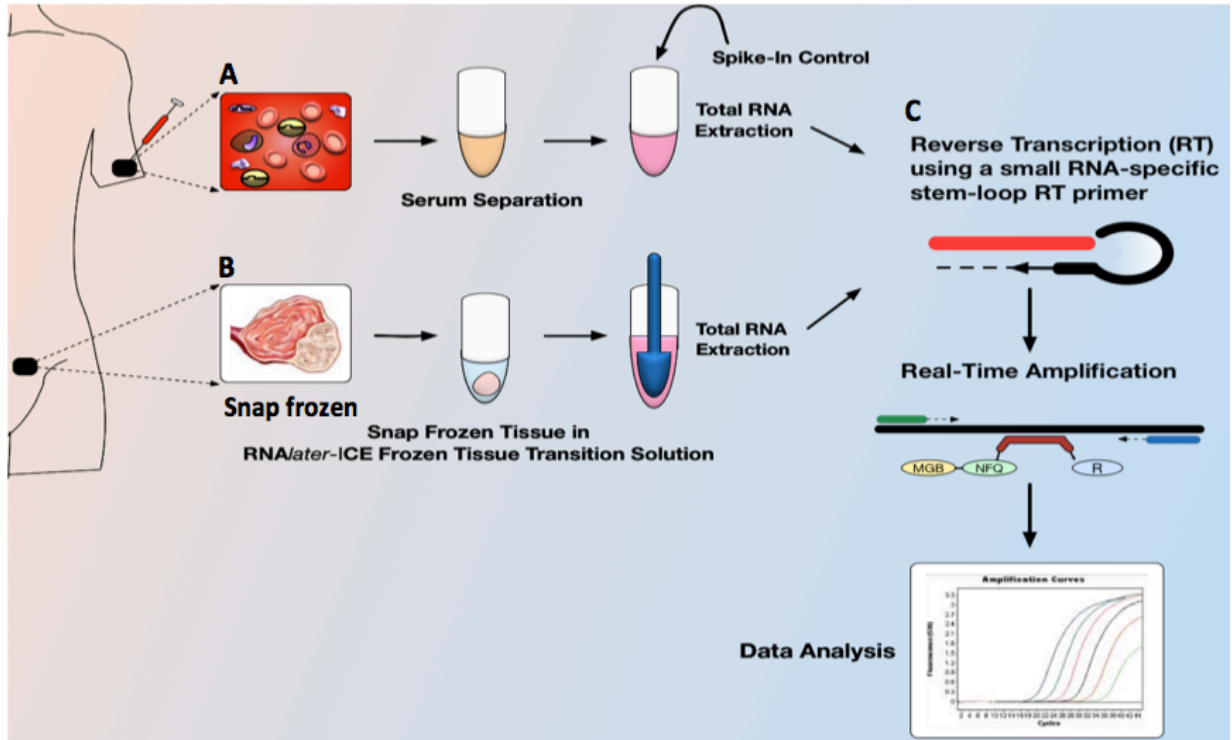


Figure 3: Schematic flow chart of the Taq-man quantitative real-time PCR experiments. A) Whole blood collection by venipuncture and serum separation, followed by RNA extraction and synthetic spike-in control was used as internal control. B) EOC tissues were snap frozen in liquid nitrogen directly after being dissected from patients, and then, placed in RNAlater-ICE Frozen tissue transition solution, followed by total RNA extraction using Triazol reagent. C) MiRNA reverse-transcription using miRNA-specific stem-loop primers and quantitative real-time PCR using TaqMan MicroRNA Assays. Figure generated using OmniGraffle 6.4.1.

CHAPTER 2 Materials and Methods

2.1 Study participants and sampling

The blood samples were collected from 13 patients with EOC prior to surgery. One blood sample from patient with benign ovarian tumor and six blood samples from age-matched healthy females with no history of cancer, were obtained as controls. The whole blood was collected by venipuncture, and then serum was separated by centrifugation at 10,000 rpm for 10 min and stored at -80°C (Figure 3).

Twenty EOC tissue samples were obtained from tumor dissection surgeries at the Oncology Center of Mansoura University starting from December 2013 till June 2015. International Federation of Gynecology and Obstetrics (FIGO) staging was used for clinical staging of the tumor. Imaging scans was obtained before surgery to determine the stage of ovarian cancer. The tumor grade was assessed through histo-pathological examination. The histo-pathological examination was performed at the oncology Center of Mansoura University. The EOC tissues were fixed with fixative solution and embedded in paraffin, then sectioned with a microtome. Dewaxed sections were stained using hematoxylin and eosin (H&E). Six healthy ovarian tissues from hysterectomy surgeries and one benign ovarian tumor were included in the study. The clinical characteristics of the patients are summarized in Table 2. The excised tissues were snap frozen, in liquid nitrogen, directly after being dissected from the patients. The snap frozen tissues were placed in RNAlater-ICE Frozen tissue transition solution and stored at -80°C . The Institutional Review Board (IRB) of the American University in Cairo approved the protocols followed in this study. All patients provided informed consents.

Table 2: Summary of the clinical characteristics of patients in the study.

Variables	OVCA Tissue Profiling Group (n=20)	OVCA Serum Profiling Group (n=13)
Age		
Mean	51	54
Minimum	30	44

Maximum	65	65
Histological Type		
Serous	18	13
Endometrioid	1	0
Mucinous	1	0
FIGO Clinical Stage		
1B	6	4
2B	1	0
3C	10	7
4	3	2
Histological Grade		
Well Differentiated (Grade-I)	11	6
Moderately Differentiated (Grade-II)	5	5
Poorly Differentiated (Grade-III)	4	2

2.2 Total RNA extraction from serum and tissue samples

RNA from the serum samples was extracted using Qiagen miRNeasy Serum/Plasma Kit (Qiagen). Frozen serum samples were allowed to thaw completely on ice and were mixed gently by inversion. Serum samples were filtered through 0.22µm filter to remove any remaining cellular contents that were not removed by centrifugation. One part of each serum sample was mixed with 5 parts of Qiazol. MiRNeasy Serum/Plasma Spike-In Control (1.6 x 10⁸ copies/µl of synthetic *C. elegans* Cel_miR-39-3P miRNA mimic 5'-UCACCGGGUGUAAAUCAGCUUG-3') was used as internal control by adding 3.5 µl of the spike-in control prior to the addition of chloroform to normalize the variation in RNA extraction and amplification efficiency between samples. The RNA extraction for serum was resumed following the manufacturer's instructions.

Total RNA was extracted from the frozen tissue samples using Triazol reagent (Invitrogen, USA) according to the manufacturer's instructions. In 1.5 ml Rnase-free Eppendorf tubes, frozen sections of the tissues were mechanically homogenized in Triazol using sterile pestles. Then after addition of chloroform, the aqueous phase was transferred into clean tube. Total RNA was precipitated using ice-cold isopropyl alcohol and pelleted by centrifugation. The formed pellet was washed, twice, with 75% ethanol. Then, the pellet was air-dried, and then re-suspended in DEPC-treated water.

The RNA concentration was assessed using the Nanodrop RiboGreen assay kit (Molecular Probes Cat. # R11490) using NanoDrop-3300 Fluoro-spectrometer (Thermo Scientific, USA). The A260/A280 ratio was measured by using spectrophotometer UV-1800 (Shimadzu, Japan) to assess the RNA purity.

2.3 Semi-quantitative reverse transcription-polymerase chain reaction (RT-PCR)

First Strand cDNA was synthesized using random primers from 1 µg RNA by RevertAid First Strand cDNA synthesis Kit (Thermo Scientific, USA) according to the manufacturer's instructions. The PCR reaction was carried out by mixing 1 µl cDNA template, 2.5 µl 10X DreamTaq PCR buffer, 0.5 µl 10mM dNTPs, 0.25 µl Dream Taq Polymerase, 0.75 µl primers (forward and reverse primers) and nuclease-free water for a total volume of 25 µl. The expression level of the genes was normalized using GAPDH as endogenous control. The thermo-cycler program is 95°C for 5 mins, followed by cycles of (95°C for 30 secs, annealing temp for 30 secs and 72°C for 45 secs). The annealing temperatures and cycle number is indicated in Table 3. We ran the PCR products on a 1.5% agarose gel then visualized using Gel Doc EZ System (Bio-Rad, USA).

Table 3: Primers used for semi-quantitative RT-PCR.

Primer	Sequence	Annealing temperature	Number of cycles
GAPDH	F*: 5'- CCACCCATGGCAAATTCCATGGCT-3' R**: 5'- TCTAGACGGCAGGTCAGGTCCACC-3'	60.5°C	30 cycles
MUCIN16/ CA125	F: 5'-ACATCAACTCCTGCCTTCCCAGAA- 3' R: 5'-	57°C	30 cycles

	ACCAGTGGGCATTCCAGAAAGAGA-3'		
CRP	F: 5'-TCGTATGCCACCAAGAGACAAGACA-3' R: 5'-AACACTTCGCCTTGCCTTCATACT-3'	58 °C	38 cycles
PAX2	F: 5'-GTACTACGAGACCGGCAGCATC-3' R: 5'-CGTTTCCTCTTCTCACCATTGG-3'	58°C	35 cycles
Vimentin	F: 5'-GAACGCCAGATGCGTGAAATG-3' R: 5'-CCAGAGGGAGTGAATCCAGATTA-3'	60 °C	35 cycles
E-Cadherin	F: 5'-CCTTCCTCCCAATACATCTCCC-3' R: 5'-TCTCCGCCTCCTTCTTCATC-3'	58°C	33 cycles
LEF1	F: 5'-ACAGCGGAGCGGAGATTACAGAG-3' R: 5'-TCCCTTGTTGTAGAGGCCTCCATC-3'	60°C	35 cycles
SOX2	F: 5'-TTACCTCTTCCTCCCACTCC-3' R: 5'-CCTCCATTCCCTCGTTT-3'	57°C	37 cycles

*Forward primer, **Reverse primer.

2.4 Quantitative real-time RT-PCR

MicroRNA-590-3p levels in the serum and tissues were analyzed using Taq-Man MicroRNA Assays (Applied Biosystems, USA). Ten ng of the total RNA was reverse-transcribed using miRNA-specific stem-loop primers and Taq-Man miRNA Reverse Transcription Kit in a scaled down 5µl reaction. The RT reactions were incubated for 30 min at 16 °C, then for 30 min at 42 °C, and then for 5 min at 85 °C. The RT products were stored at -20 °C till running the real-time PCR reaction. The real-time PCR reaction was performed using Taq-Man MicroRNA Assays (Table 4) (Reporter dye: FAM and reporter quencher: NFQ) on Mx3005P QPCR System (Stratagene). The cDNA was mixed with the PCR primers and probes (5'-FAM and 3'-TAMRA), and Taq-Man Universal Master Mix, No AmpEraseH UNG (Applied Biosystems), then incubated at 95 °C for 10 min, followed by 40 cycles of 95°C for 15 sec and 60°C for 1 min. Automatic setting for assigning the baseline and threshold for Ct determination was used. A Ct of 35 was set as cut-off value to be considered as non-detected (Caraguel et al., 2011). For the serum samples, Synthetic *C. elegans* Cel_miR-39 miRNA mimic was used as internal control (validated control by (Zhang et al., 2013)). The expression level of the tissue miR-590-3p was normalized to U6 snRNA. Each measurement was performed in duplicates including the no-template controls and the no-reverse transcriptase controls. The relative

quantification of miR-590-3p was estimated using the comparative $\Delta\Delta\text{CT}$ method (Livak & Schmittgen, 2001).

Table 4: Taq-Man MicroRNA Assays

MicroRNA Accession Number	MicroRNA Assay Name	Assay ID	MicroRNA sequence
MIMAT0004801	Hsa-miR-590-3p	002677	UAAUUUUAUGUAUAAGCUAGU
NR_004394	U6 snRNA	001973	GTGCTCGCTTCGGCAGCACATAT ACTAAAATTGGAACGATACAGAG AAGATTAGCATGGCCCCTGCGCA AGGATGACACGCAAATTCGTGAA GCGTTCATATTTT
MIMAT0000010	Cel-miR-39	000200	UCACCGGGUGUAAAUCAGCUUG

2.5 Western blot analysis

Protein lysates were prepared by mechanical homogenization of the tissues in 2X ice-cold Laemmle lysis buffer (50mM Tris pH6.8, 2% sodium dodecyl sulfate (SDS), and 10% glycerol) with freshly added 1X Halt Protease Inhibitor Cocktail (ThermoScientific, USA). Then, the samples were incubated at 4°C for 2 hours, followed by centrifugation at 12,000 rpm at 4°C for 20 minutes. The supernatant protein lysates were transferred into fresh Eppendorf tubes and quantified using Pierce BCA Protein Assay Kit (Pierce Biotechnology, USA) according to the manufacturer's instructions. Serial dilution of the standard bovine serum albumin (BSA) of known concentration was prepared to generate the standard curve. Optical density was taken at 562nm using spectrophotometer and the working reagent was used as a blank.

Equal concentrations of the protein lysates (30 μ g) were mixed with 6X SDS-Laemmli loading dye (60% Glycerol, 360 mM Tris-HCl pH 6.8, 12% SDS, 0.06% bromophenol blue, 30% beta-mercaptoethanol) and boiled at 99°C for 5 minutes. The samples were loaded on 12% SDS- polyacrylamide gel, and then plotted on a PVDF membrane. After blocking the membrane with 5% nonfat dry milk in PBS with 0.01% Tween 20 for 1

hour, the membrane was incubated with anti-SOX-2 rabbit polyclonal antibody (0.5µg/ml), or anti-LEF1 goat polyclonal antibody (2µg/ml) overnight at 4°C. After washing, we incubated the membrane in goat anti-rabbit or mouse anti-goat alkaline phosphatase-conjugated secondary antibody (KPL) (1:10000 dilution in 5% non-fat dry milk in PBS-T). After washing, the protein bands were detected using Phosphatase Chemiluminescent Substrate.

To examine the loading control on the same membranes, the membranes were incubated with harsh stripping buffer (0.5 M Tris-HCl, 10% SDS and beta-mercaptoethanol) for 15 minutes at 65°C, then washed thoroughly with water to remove any traces of beta-mercaptoethanol. The membranes were blocked with blocking solution for one hour, then incubated with anti-β-Tubulin mouse monoclonal antibody (Sigma, T7816) (1:20,000 in 5% non-fat dry milk) overnight at 4°C. After washing, we incubated the membrane in goat anti-mouse alkaline phosphatase-conjugated secondary antibody (KPL) (1:10000 in 5% non-fat dry milk in PBS-T). After washing, the protein bands were detected using Phosphatase Chemiluminescent Substrate.

2.6 Target gene prediction and miRNA function prediction analysis

MiR-590-3p potential target genes were predicted using TargetScan (Agarwal et al., 2015) (www.targetscan.org), and miRanda-mirSVR (Betel et al., 2010; Betel et al., 2008; John et al., 2004) (www.microrna.org). The thermodynamic stability between miR-590-3p and the 3'UTR of LEF1 mRNA and PAX2 mRNA was predicted using miRmap (<http://mirmap.ezlab.org/app/>). The expression profiles of the potential target genes were examined using Oncomine data-mining platform (<http://www.oncomine.org>) (Rhodes et al., 2004) that covers cancer microarrays. StarBase Pan-cancer analysis platform (http://starbase.sysu.edu.cn/pan_Cancer.php) (Li et al., 2014; J.-H. Yang et al., 2011) was used to compile the expression profiles of miR-590-3p and LEF1 utilizing the data available at The Cancer Genome Atlas (TCGA) Data Portal and to study the correlation between their expression levels in ovarian cancer.

We used FAME (Functional Assignment of MicroRNAs via Enrichment) software (Ulitsky et al., 2010) (<http://acgt.cs.tau.ac.il/fame/>) to predict the potential function of miR-590-3p through analyzing its downstream target genes.

2.7 Statistical analysis

The relative expression of miR-590-3p was calculated using the comparative $\Delta\Delta\text{CT}$ method (Livak & Schmittgen, 2001). The relative levels of miR-590-3p were presented as log transformed $\log_{10}(2^{-\Delta\Delta\text{CT}})$ of the relative levels of miR-590-3p. Serum miR-590-3p levels were used to generate the receiver operating characteristic (ROC) area under the curves (AUC) to study the ability of miR-590-3p to distinguish between the EOC patients and healthy females. Linear regression analysis was used to analyze the correlation between miR-590-3p levels and the levels of the potential down-stream target genes. ImageJ software (<http://www.imagej.nih.gov/ij>) was used for densitometric analysis to analyze the results of the semi-quantitative PCR and the western blot and for normalization to the endogenous control. Data are presented as mean \pm standard Deviation (SD). For statistical comparisons, the The Mann–Whitney test was carried out. A probability value (P-value) <0.05 was considered to indicate statistical significance. One-way ANOVA (with Bonferroni post-test) was carried out to analyze the difference between multiple experimental groups with a single variable. Statistical analyses were performed using GraphPad Prism 6 statistical packages.

CHAPTER 3 Results

3.1 Clinico-pathologic Characteristics

The blood samples were collected from 13 patients prior to surgery, four patients at early stage (stage I/II) and nine patients at advanced stage (stage III/IV) (Table 2). Six blood samples were collected from healthy females with no history of cancer and one obtained from a patient with benign ovarian tumor. The EOC tissue samples were collected from 20 patients. The clinical characteristics of the patients are summarized in Table 2 and 5. The clinical stage distribution among the enrolled patients for tissue sampling is six patients (30%) at stage-I, one patient (5%) at stage-II, ten patients (50%) at stage-III and three patients (15%) at stage-IV. We examined the histological grade of the EOC tissues. Eleven samples (55%) were characterized as well differentiated grade-I, five (25%) as moderately differentiated grade-II and four (20%) EOC samples as poorly differentiated grade-III (Figure 4). Different histological subtypes of EOC were involved including serous EOC, which represents 18 cases, and also endometrioid and mucinous EOC were included. The mean age of EOC patients is 51 (age range 30-65) years. The control ovarian tissues were collected from 6 healthy controls with no history of cancer from hysterectomy surgeries, and one patient with benign ovarian tumor, with mean age of 55 years (age range 50-63).

Table 5: Clinical characteristics of EOC patients in the study.

Sample ID	FIGO Stage	Histological Grade	CA 125 (U/ml)	Pre-operative chemotherapeutic treatment	Metastasis at diagnosis
C1	III C	Grade-I	430	Treated	Metastasis to lymph
C2	IIB	Grade-III	220	Treated	No Metastasis
C3	III C	Grade-I	>600	Not Treated	
C4	IB	Grade-I	470	Not Treated	
C5	III C	Grade-I	116	Not Treated	

C6	IB	Grade-III	>600	Treated	No Metastasis
C7	1B	Grade-I	6.15	Not Treated	
C8	IV	Grade-III	7	Not Treated	
C9	IB	Grade-I	10	Not Treated	No Metastasis
C10	IV	Grade-III	533	Treated	Metastasis to lymph
C11	IIIC	Grade-II	97	Treated	No Metastasis
C12	IB	Grade-I	79	Treated	
C13	IB	Grade-I	48	Not Treated	
C14	IIIC	Grade-II	>600	Treated	Metastasis
C15	IV	Grade-II	>600	Not Treated	No Metastasis
C16	IIIC	Grade-I	90	Not Treated	
C17	IIIC	Grade-II	70	Not Treated	
C18	IIIC	Grade-II	110	Not Treated	
C19	IIIC	Grade-I	>600	Not Treated	
C20	IIIC	Grade-I	>600	Not Treated	
CS*-1	IIIC	Grade-III	>600	Treated	Metastasis
CS-2	IB	Grade-I	>600	Not Treated	No Metastasis

* Cancer serum (Serum specimens only)

Table 6: The levels of tissue *CRP* in different stages of EOC

FIGO Stage	Tissue <i>CRP</i> mRNA Levels	EOC Samples
IB	Absent	-
	Low	C6, C7, C9, C4
	High	C12, C13
IIB	Absent	-
	Low	C2
	High	-
IIIC	Absent	C20
	Low	C5, C14, C16, C19
	High	C1, C3, C11, C17, C18,

IV	Absent	-
	Low	C8
	High	C10, C15

Table 7: The levels of tissue *PAX2* in different histological grades.

Histological Grade	Tissue <i>PAX2</i> mRNA Levels	EOC Samples
Grade-I	Absent	C3, C7, C9, C12, C13, C16, C20
	Low	C4, C19
	High	C1, C5
Grade-II	Absent	C11, C14, C15, C17, C18
	Low	-
	High	-
Grade-III	Absent	C2, C6, C8, C10
	Low	-
	High	-

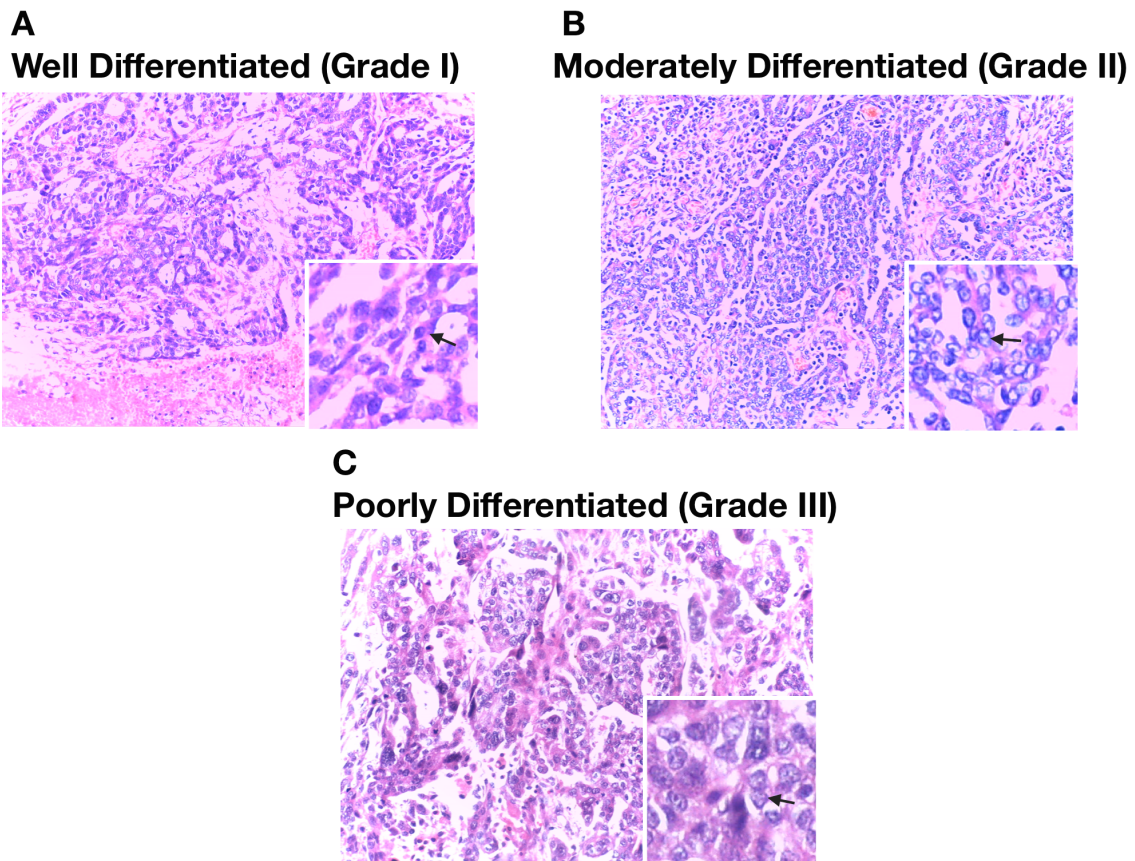


Figure 4: Histological grade of EOC samples. The figure shows representative samples from each histological grade **A)** A well-differentiated grade-I sample with uniform, small, and round to oval nuclei. **B)** The grade-II sample was characterized by uniform nuclei that are larger than that of the low-grade but smaller than the high-grade nuclei. **C)**

The high-grade nuclei are larger with greater pleomorphism and increased nuclear-to-cytoplasmic ratio. The insets at higher magnification highlight the nuclear features at different grades (indicated by an arrow). (Hematoxylin and Eosin stains).

3.2 Histo-pathological characterization at the molecular level

Intra-tumoral heterogeneity of cellular phenotypes is a challenging factor in the assessment of the histo-pathological characters of the tumor and correlating the levels of biomarkers to the tumor features. The heterogeneity of cellular phenotype within the tumor mainly stems from the gradient level of differentiation within neoplasms, the different levels of interactions between tumor cells via intercellular vesicles (exosomes), and the effect of the microenvironment on the tumor cells (Fidler & Hart, 1982). To perform a reliable correlation between miR-590-3p levels and the tumor characteristics, we analyzed the histo-pathological features at the molecular level via examining the mRNA steady-state levels of molecular biomarkers using RT-PCR. So that, the same aliquot is being examined for the levels of biomarkers related to the histo-pathological status of the tumor, as well as the levels of miR-590-3p. We examined the expression of various acknowledged biomarkers including *CA125/Mucin16* which is being used for EOC screening (Høgdall et al., 2007) and C-reactive protein (*CRP*) which expression was correlated with the stage of the disease, as higher expression of *CRP* was associated with late stages of EOC (Hefler-Frischmuth et al., 2009). And, paired homeobox 2 (*PAX2*) gene expression, which was found to show different expression levels in low-grade versus high grade EOC, was used as a marker for the EOC grade (Tung et al., 2009).

The average CA125/Mucin16 blood level of the cases in the study is ≈ 290 U/ml (n=20). 85% of patients exhibited high CA125/Mucin16 blood levels (above the normal threshold 35U/ml), whereas the other 15% of patients (C7, C8 & C9) had normal levels of blood CA125/Mucin16, despite being diagnosed with OVCA (Table 5). At the level of tissue expression, the tissue mRNA steady-state levels of CA125/Mucin16 were elevated in about 70% of the EOC tissue samples. Its levels were low in six EOC samples including four samples from patients subjected to platinum-based combination chemotherapy (C1, C2, C6, C10) (Figure 5). As expected the tissue mRNA steady-state level of CRP were associated with the clinical stages of EOC. Higher levels of CRP were observed at advanced stages of EOC, relative to the early-stage EOC, except for two early-stage EOC

samples (C12&C13) that showed high levels of CRP (Table 6) (Figure 6). In agreement with what has been reported in the literature (Tung et al., 2009), high PAX2 tissue mRNA levels were observed in the majority of low-grade EOC (C1, C4, C5 and C19) and PAX2 expression was completely diminished in high-grade EOC (C2, C6, C8, C10, C11, C14, C15, C17, and C18) (Table 7) (Figure 7). The abolished PAX2 expression in the ovarian mucinous carcinoma (C7) is in accord with previous studies that detected PAX2 expression in ovarian serous and endometrioid carcinoma, but not in the ovarian mucinous carcinoma (Schaner et al., 2003; Wang et al., 2015).

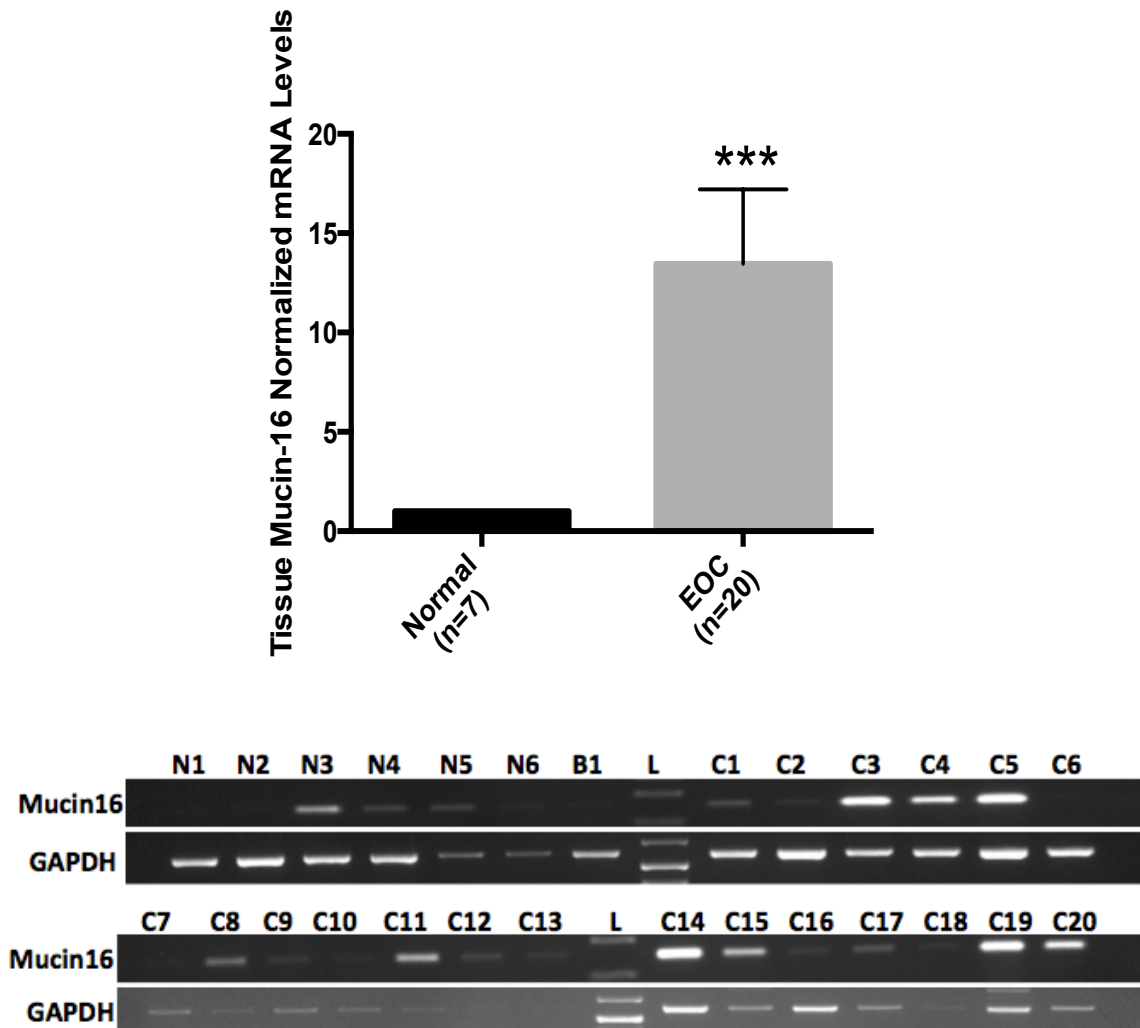


Figure 5: RT-PCR analysis of tissue *CA125/Mucin16* shows elevated levels in EOC relative to control tissues ($P=0.0001$). The intensities of the semi-quantitative PCR bands were normalized to the endogenous control *GAPDH* using ImageJ. N1 –N6 represent healthy ovarian tissues, B1 is benign tumor and C1-C20 represent EOC samples. (*) $P<0.0005$)**

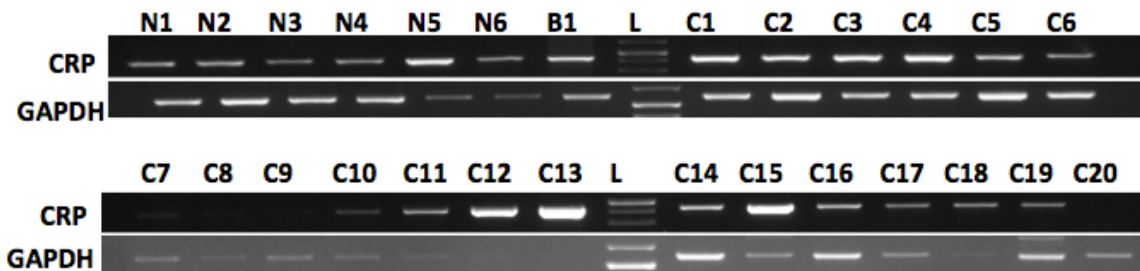
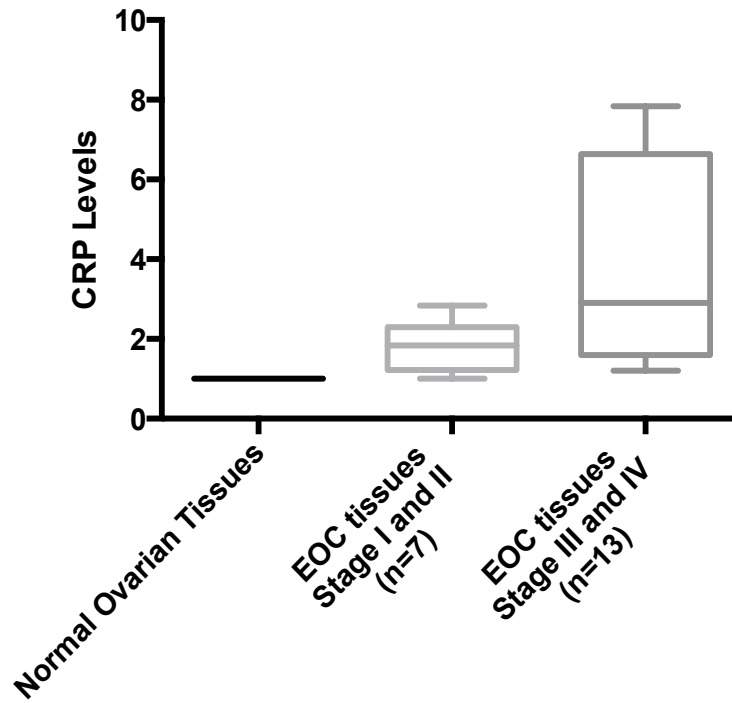


Figure 6: Higher levels of *CRP* were associated with advanced stages of EOC. The early-stage EOC samples are C2, C4, C6, C7, C9, C12, and C13. However, C1, C3, C5, C8, C10, C11, C14, C15, C16, C17, C18, C19 and C20 are late-stage EOC. The intensities of the semi-quantitative PCR bands were normalized to the endogenous control *GAPDH* using ImageJ. N1 –N6 represent healthy ovarian tissues, B1 is benign tumor and C1-C20 represent EOC samples.

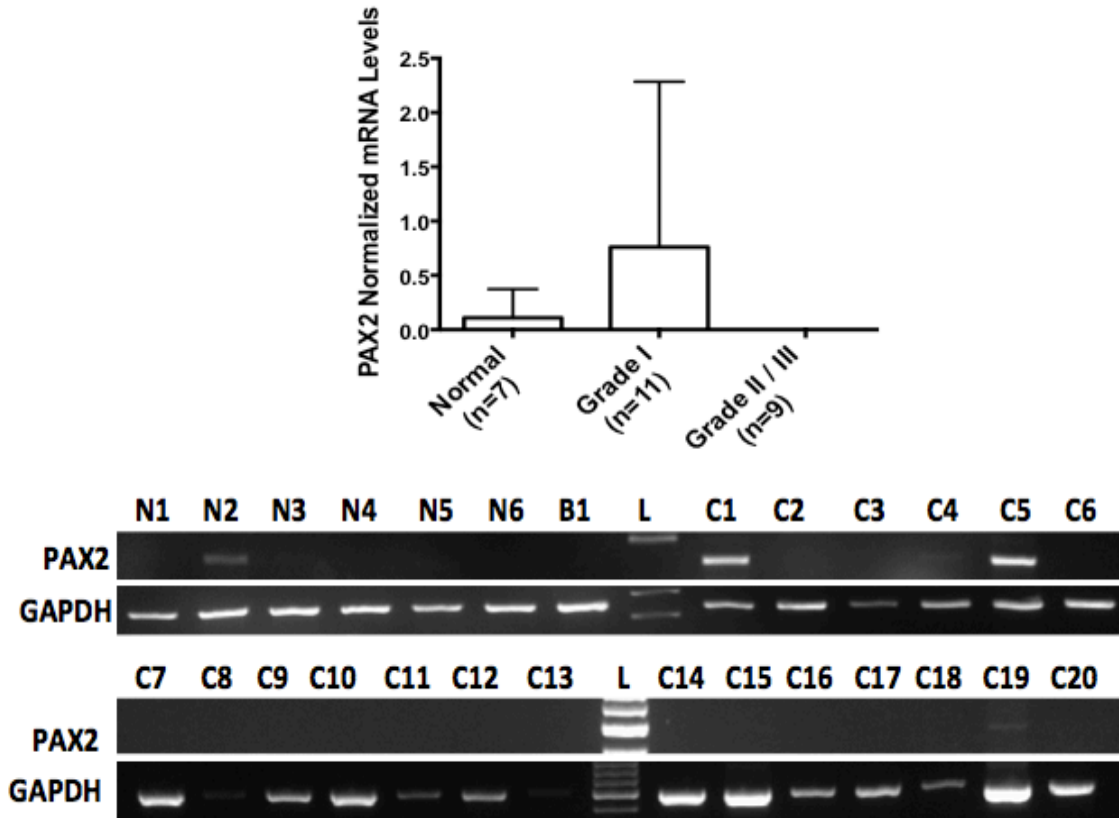


Figure 7: The level of *PAX2* mRNA in EOC samples is a marker for EOC histological grade. The histological low-grade EOC samples are C1, C3, C4, C5, C7, C9, C12, C13, C16, C19 and C20. The histological higher-grade (grade-II/III) samples are C2, C6, C8, C10, C11, C14, C15, C17, and C18. *PAX2* expression was completely diminished in high-grade EOC.

3.3 Upregulation of serum miR-590-3p in EOC patients

We examined the expression levels of miR-590-3p in the serum of 13 EOC patients, and 7 controls using qRT-PCR. The levels of miR-590-3p in the serum of EOC patients (84.6%) were significantly higher than that of the healthy controls ($P=0.04$) (Figure 8). Interestingly, the levels of miR-590-3p in C9 that showed normal level of pre-operative blood CA125/Mucin16 (below 35U/ml) was significantly elevated compared to healthy controls. We analyzed the correlation between miR-590-3p serum levels and the clinico-pathological features of EOC. The patients were categorized into two groups according to the stage, the early-stage group (stage I/II, $n=4$) and late-stage group (stage III/IV, $n=9$), and two groups according to the tumor differentiation grade, group of histological grade-I ($n=6$) and group of histological grade-II/III ($n=7$). We found that there was no significant difference in the serum miR-590-3p levels between the different stages (Figure 9A).

Likewise, no significant difference was observed among the patients with different tumor differentiation grade (Figure 9B). Also, receiving pre-operative chemotherapeutic treatment didn't affect serum miR-590-3p levels (Figure 9C). Additionally, there was no significant correlation between serum miR-590-3p and metastasis (Figure 9D). It is worth noting that we were limited to the small sample size of metastasis cases (n=3).

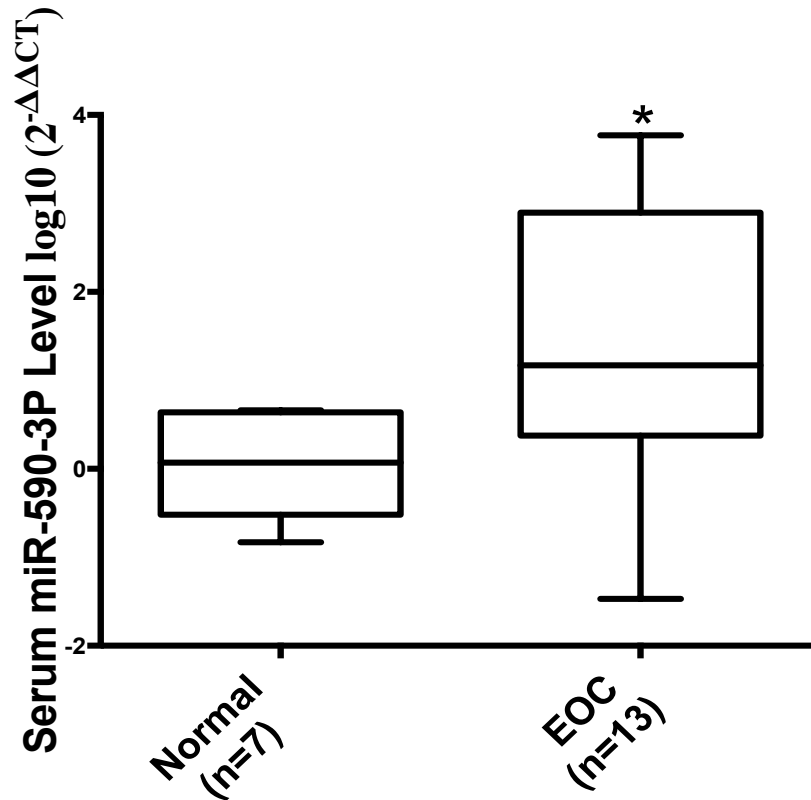


Figure 8: miR-590-3p is significantly elevated in EOC patients' serum. Box plot represents serum miR-590-3p expression levels in controls and EOC patients. The level of serum miR-590-3p was normalized to the synthetic *C. elegans* Cel_miR-39 Spike-in control. The upper and lower borders of the boxes indicate the 75th and 25th percentiles, respectively. The whisker caps indicate the 90th and 10th percentiles. The horizontal lines in the boxes indicate the median values. P-value was depicted using the Mann-Whitney U-test. The relative levels of miR-590-3p are presented as log transformed $\log_{10}(2^{-\Delta\Delta CT})$ of the relative levels of miR-590-3p. (* P<0.05)

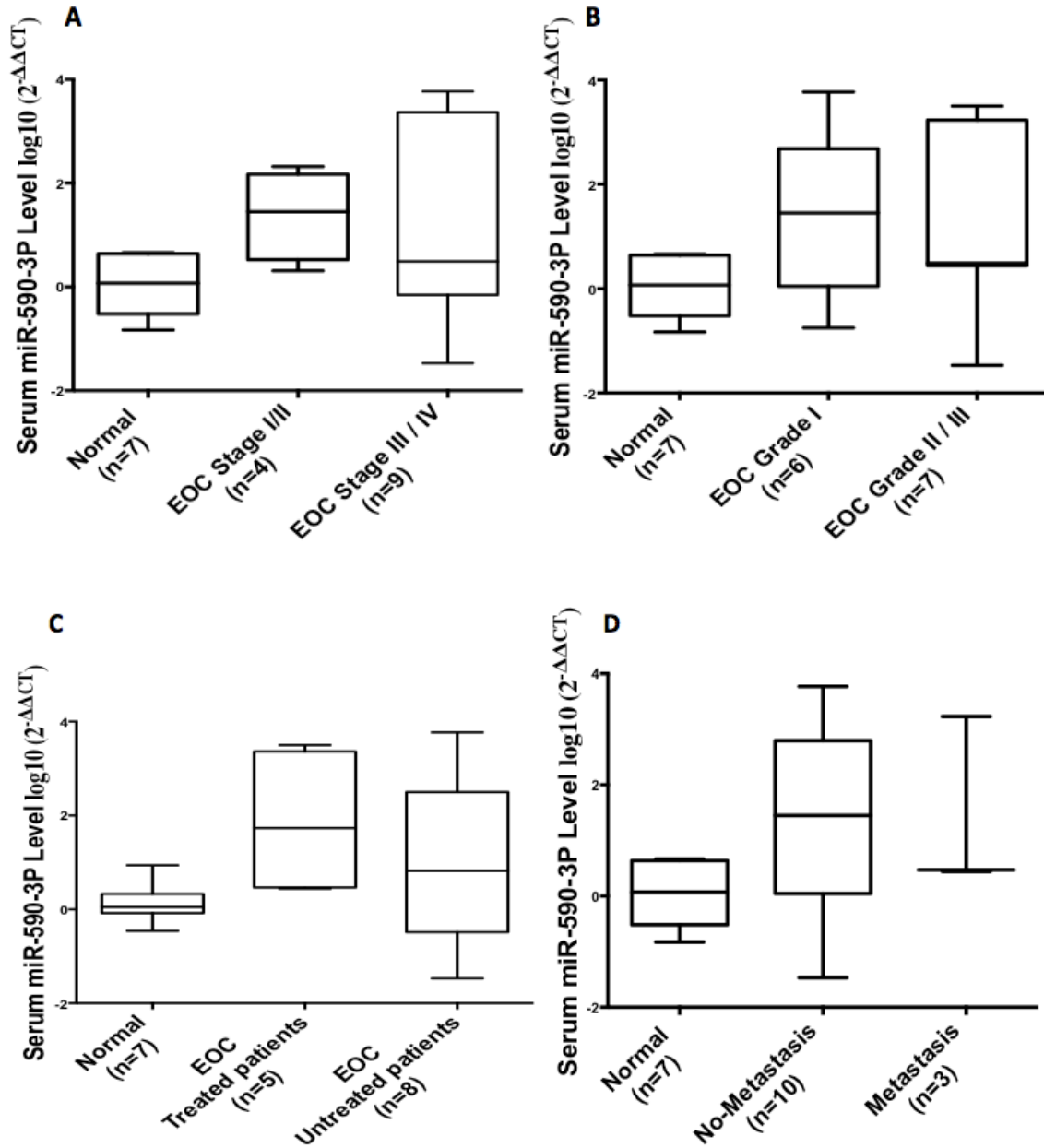


Figure 9: The correlation between serum miR-590-3p levels and EOC clinico-pathological features. (A) Serum miR-590-3p did not significantly differ among EOC patients with different clinical stages, (B) or in EOC patients with different histological grades. (C) Serum miR-590-3p levels were not affected by pre-operative chemotherapeutic treatment, (D) and showed no significant correlation with the existence of metastasis. The upper and lower borders of the boxes indicate the 75th and 25th percentiles, respectively. The whisker caps indicate the 90th and 10th percentiles. The horizontal lines in the boxes indicate the median values. One-way ANOVA (with Bonferroni post-test) was carried out to analyze the statistical significance. ($P > 0.05$)

3.4 Serum miR-590-3p level is a promising diagnostic marker for epithelial ovarian cancer

We performed the Receiver-operator characteristic (ROC) curve analysis to study the specificity and sensitivity of circulating miR-590-3p to assess its ability to distinguish between EOC patients and healthy females. When comparing between serum miR-590-3p levels in EOC patients and healthy controls, the area under the ROC curve (AUC) was 0.76 with 95% confidence interval (CI) of 0.54–0.97 and P-value= 0.05 (Figure 10). Serum miR-590-3p optimal cut-off value of 2.4 for the $2^{-\Delta\Delta CT}$ had 76.92% sensitivity and 71.4% specificity (95%CI=46.19% to 94.96%). We examined the diagnostic ability of serum miR-590-3p for stage-I ovarian cancer patients (n=4) versus healthy controls (n=7) and the best cutoff value at 4.4 of the $2^{-\Delta\Delta CT}$ showed 75% sensitivity and 85.71% specificity (95%CI=42.13% to 99.64%). The best cutoff value for stage-III/IV patients (n=9) versus healthy controls (n=7) was $2^{-\Delta\Delta CT}$ of 2.4 with 77.78% sensitivity and 71.43% specificity (95%CI=40% to 97.1%). On the other hand, as expected from the above results, circulating miR-590-3p could not be used to distinguish between EOC patients with different clinical stage or tumor differentiation grade. Therefore, our results suggest that circulating miR-590-3p is a promising biomarker for diagnosis of early-stage EOC.

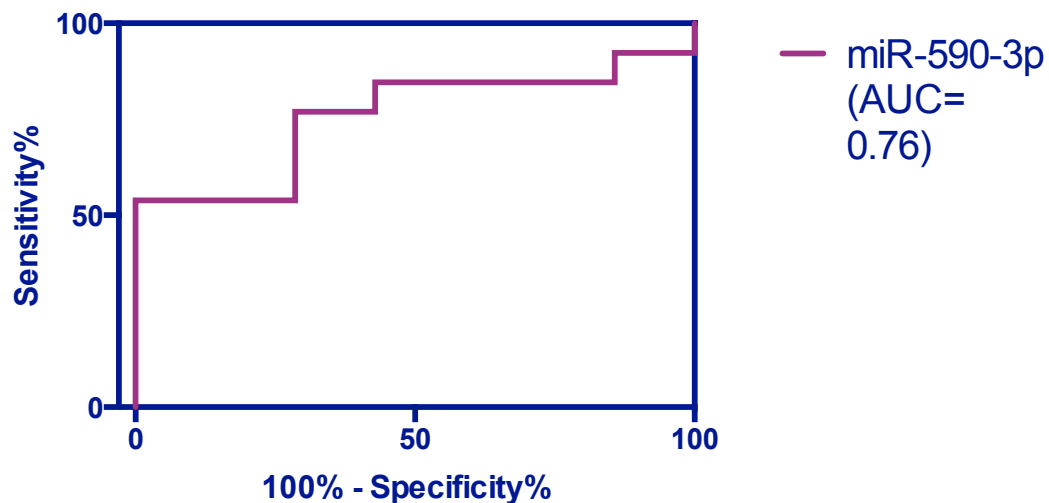
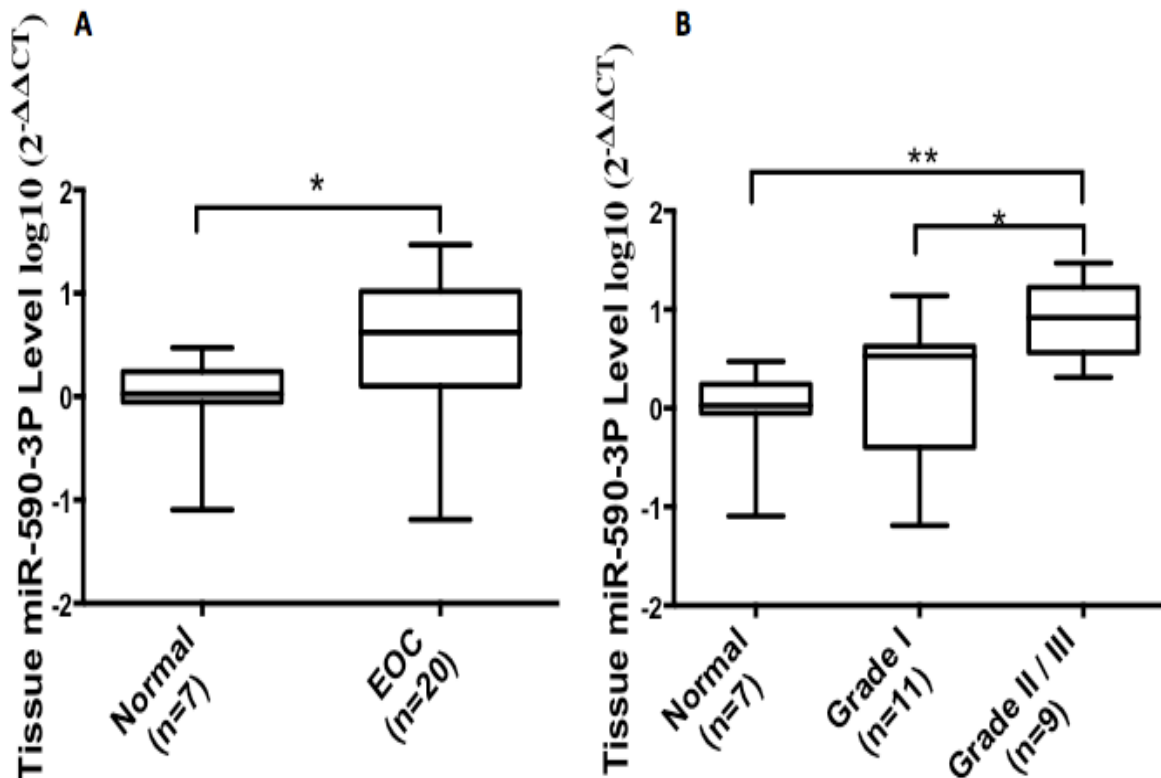


Figure 10: Receiver-operator characteristics (ROC) curve analyses of circulating miR-590-3p for EOC patients versus healthy controls. Circulating miR-590-3p yielded AUC of 76% (P-value= 0.05) with 76.92% sensitivity and 71.4% specificity at its optimal cutoff value.

3.5 Upregulation of miR-590-3p in EOC tissues

To study whether the level of serum miR-590-3p corresponds to its expression in EOC tissues, we examined the levels of miR-590-3p in 20 EOC tissues, as well as six healthy ovarian tissues and one benign ovarian tumor using qRT-PCR. And the level of miR-590-3p was normalized to U6 snRNA. The expression levels of miR-590-3p were significantly elevated in 75% of EOC tissues compared to the benign tumor and the healthy ovarian tissues ($P < 0.05$, Figure 11A). Among the 20 EOC samples, 15 samples showed elevated miR-590-3p. The level of miR-590-3p was significantly elevated in high-grade poorly differentiated EOC (grade II/III) (Figure 11B). Whereas four out of the five EOC with low miR-590-3p levels are low-grade well-differentiated EOC. There was no significant correlation between tissue miR-590-3p levels and stage, preoperative chemotherapeutic treatment or existence of metastasis (Figure 11 C, D & E). We did not study the correlation of miR-590-3p levels with progression-free interval or survival due to the recent diagnosis of the disease among the enrolled participants.



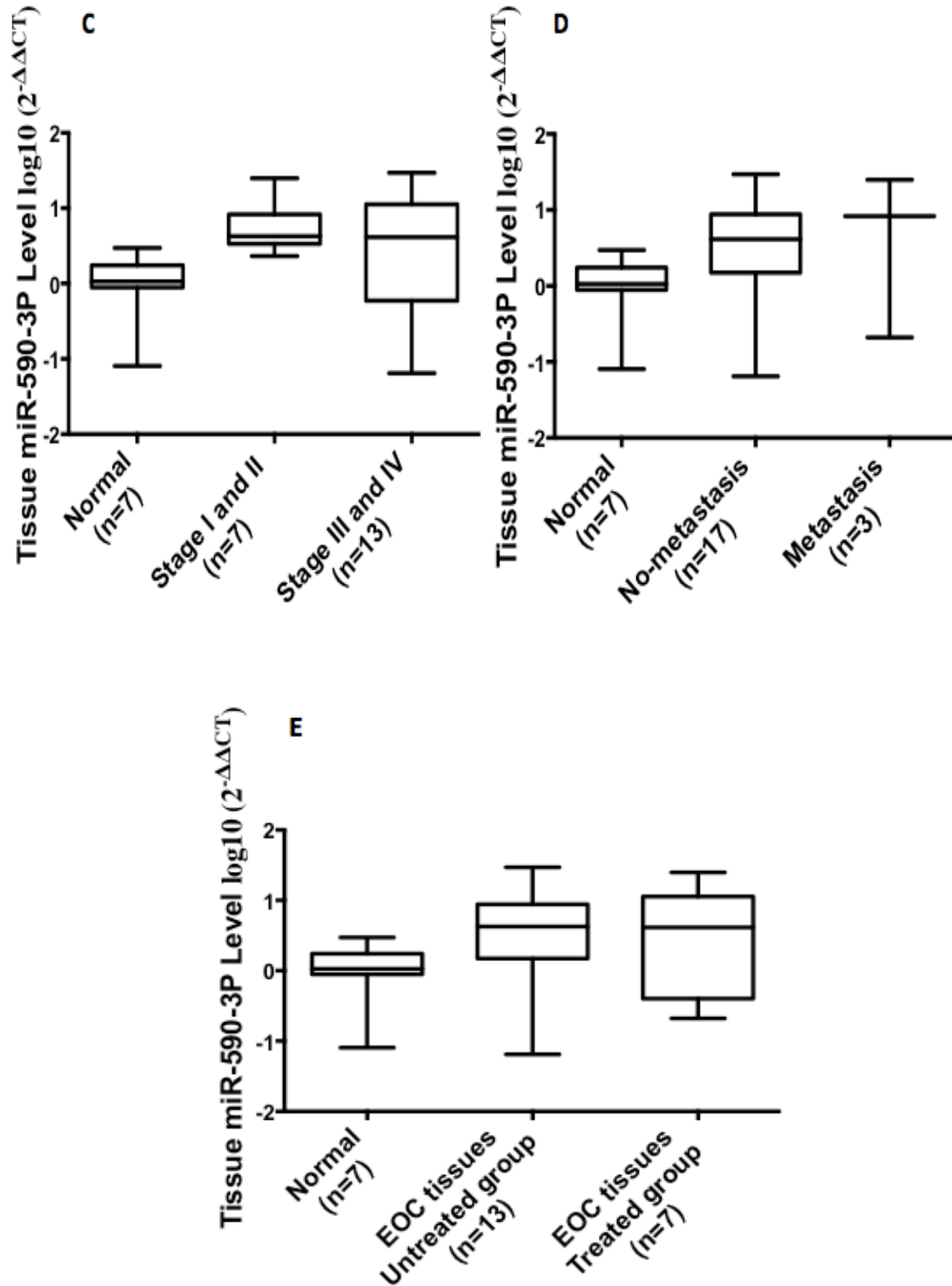


Figure 11: MiR-590-3p expression in EOC tissues. A) MiR-590-3p is significantly elevated in EOC tissues compared to controls. B) Significant correlation of tissue miR-590-3p with high grade EOC. The tissue levels of miR-590-3p didn't significantly differ

among C) different stage, D) existence of metastasis or E) pre-operative chemotherapeutic treatment. The relative levels of miR-590-3p are presented as log transformed $\log_{10}(2^{-\Delta\Delta CT})$. The upper and lower borders of the boxes indicate the 75th and 25th percentiles, respectively. The whisker caps indicate the 90th and 10th percentiles. The horizontal lines in the boxes indicate the median values. (*P<0.05, **P<0.005)

3.6 The correlation between miR-590-3p levels and epithelial–mesenchymal transition (EMT) in EOC

We were limited by the small size of metastatic samples (n=3), to effectively study the correlation between miR-590-3p and metastasis. Nonetheless, the above finding (Figure 11B) that reveals the correlation between tissue miR-590-3p and poorly differentiated EOC triggered us to further study the role of miR-590-3p in EOC tumorigenesis. We studied the correlation between miR-590-3p levels and EMT in EOC by examining the mRNA steady-state levels of EMT- related markers (the epithelial marker E-cadherin and the mesenchymal marker Vimentin) in EOC and control tissues. We divided the EOC tissue samples into two groups, a high miR-590-3p group and low miR-590-3p group. The group with high miR-590-3p indicates miR-590-3p levels more than two folds of that of the control and the remaining samples were categorized in the low-miR-590-3p group. We observed a correlation between the expression of miR-590-3p and the molecular changes of EMT in EOC (Figure 12). As, elevated levels of the mesenchymal marker Vimentin was observed in the EOC samples with high miR-590-3p levels indicating that miR-590-3p could have a role in EMT in EOC.

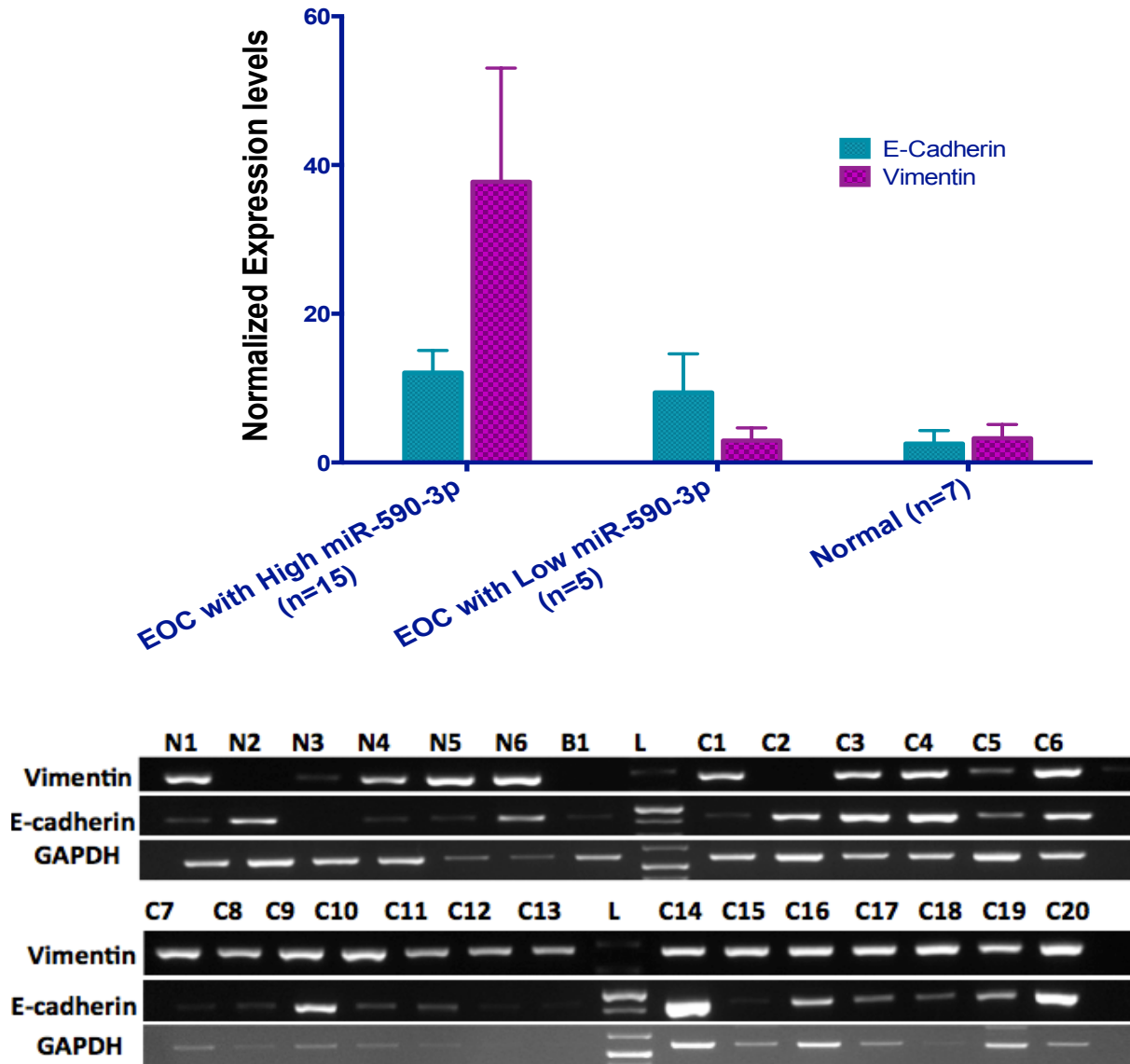


Figure 12: The mRNA steady state levels of EMT markers in EOC and control ovarian tissues. The epithelial marker E-cadherin and the mesenchyme marker Vimentin mRNA levels were examined using RT-PCR. The band intensities were normalized to the endogenous control *GAPDH* using ImageJ. The level of the mesenchymal marker Vimentin is elevated in the high miR-590-3p expressing EOC samples relative to the low-miR-590-3p group (C1, C3, C5, C14 and C20).

3.7 Bioinformatics analysis of miR-590-3p potential target genes

MicroRNAs acquire their function via post-transcriptional regulation of their target genes. Therefore, to gain an insight to the function of miR-590-3p, we analyzed the function of its downstream targets. We performed functional prediction analysis of miR-590-3p using FAME software (Ulitsky et al., 2010) and it showed that its target genes

were significantly enriched in different biological pathways including oligodendrocyte differentiation (P=0.0002), RNA splicing (P=0.0007), glial cell differentiation (0.01), metanephros development (0.02) and spermatid differentiation (P=0.03). This indicates that the upregulation of miR-590-3p in EOC plays a role in carcinogenesis through disrupting key biological processes.

To study the effect of miR-590-3p upregulation on its downstream target genes in EOC, we performed bioinformatics analysis to predict the potential target genes of miR-590-3p, utilizing TargetScan (Agarwal et al., 2015), and miRanda-mirSVR (Betel et al., 2010; Betel et al., 2008; John et al., 2004) target prediction tools. In miRanda-mirSVR target prediction tool, miRanda depicts the potential target genes based on the complementation between the seed sequence of the miRNA and its target mRNA and mirSVR score the alignment based on the miRNA-mRNA duplex base pairing, the A/U content around the seed sequence, the mRNA accessibility and the conservation. Also, TargetScan demonstrates the conservation of the target sequence, as well as the sequence features, including the A/U content, seed region pairing and the location of the target site within the 3'UTR of the target gene.

SOX2 was identified to be a potential target gene by miRanda-mirSVR with a single target site for miR-590-3p (Table 8). *LEF1* and *PAX2* were predicted as downstream targets by both TargetScan (Agarwal et al., 2015), and miRanda (Betel et al., 2010; Betel et al., 2008; John et al., 2004) (Table 8). Where, *LEF1* 3'UTR has two potential binding sites and *PAX2* 3'UTR encompasses three potential binding sites for miR-590-3p. The binding sites with the highest miRNA-mRNA thermodynamic stability are presented in Table 8. *LEF1* target region is conservative among three species of mammals (Homo sapiens, Macaca mulatta, Bos Taurus) (Figure 14) and the target region within *PAX2* 3'UTR is conserved among various species of mammals (Figure 15A). The thermodynamic stability between miR-590-3p and the 3'UTR of *LEF1* mRNA or *PAX2* mRNA was calculated using miRmap, which predicted the minimum free energy of the miRNA:mRNA duplex (Table 8), and the accessibility of the target region to the miRNA-RISC complex (Table 8).

We, then, filtered the potential target genes through assessing their expression profiles using Oncomine data-mining platform (<http://www.oncomine.org>) (Rhodes et al., 2004) and StarBase Pan-cancer analysis platform (http://starbase.sysu.edu.cn/pan_Cancer.php) (Li et al., 2014; J.-H. Yang et al., 2011). The correlation between the expression profiles of miR-590-3p and *LEF-1* retrieved from the data available at the cancer genome atlas (TCGA) Data Portal using StarBase Pan-cancer analysis platform (Li et al., 2014; J.-H. Yang et al., 2011) showed significant negative correlation between their expression levels in ovarian cancer. Moreover, the microarray dataset from Bonome study (Bonome et al., 2008), obtained from Oncomine data-mining platform, showed significant downregulation of *LEF1* in ovarian cancer relative to normal ovarian tissues (Figure 14C). Similarly, The datasets obtained from the cancer genome atlas (TCGA) ovarian cancer gene expression data showed significant downregulation of *PAX2* in ovarian cancer compared to normal ovaries (Figure 15B), suggesting a negatively correlation between miR-590-3p and *PAX2* expression in ovarian cancer.

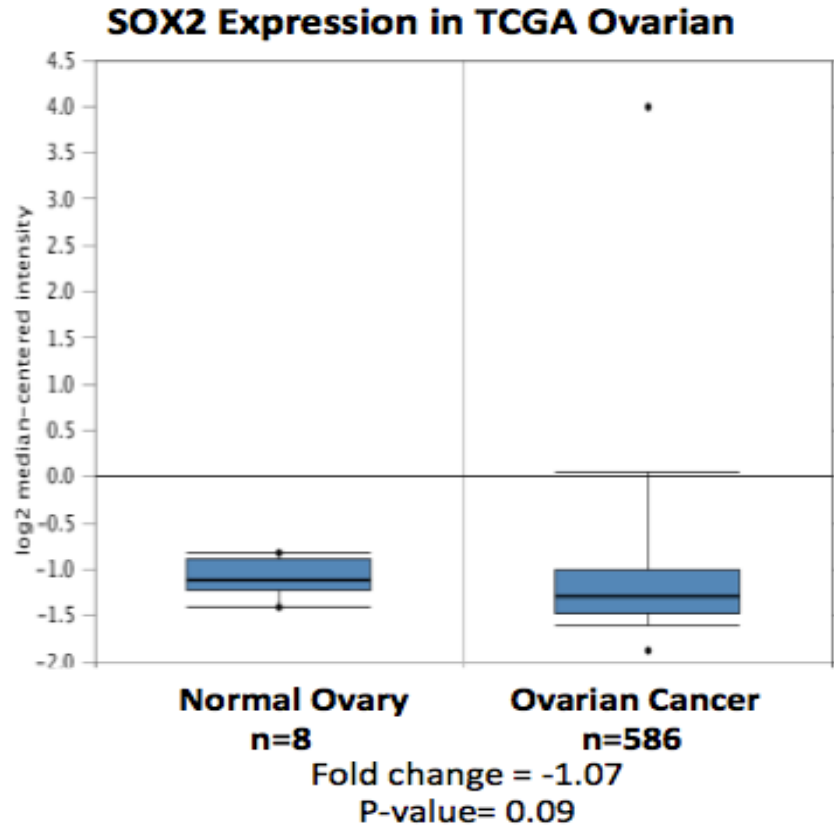


Figure 13: Downregulation of *SOX2* in ovarian cancer relative to normal ovarian tissues. The datasets were retrieved from the cancer genome atlas (TCGA) Data Portal using OncoPrint cancer database. The upper and lower borders of the boxes indicate the 75th and 25th percentiles, respectively. The whisker caps indicate the 90th and 10th percentiles. The horizontal lines in the boxes indicate the median values and the dots represent the minimum and maximum values.

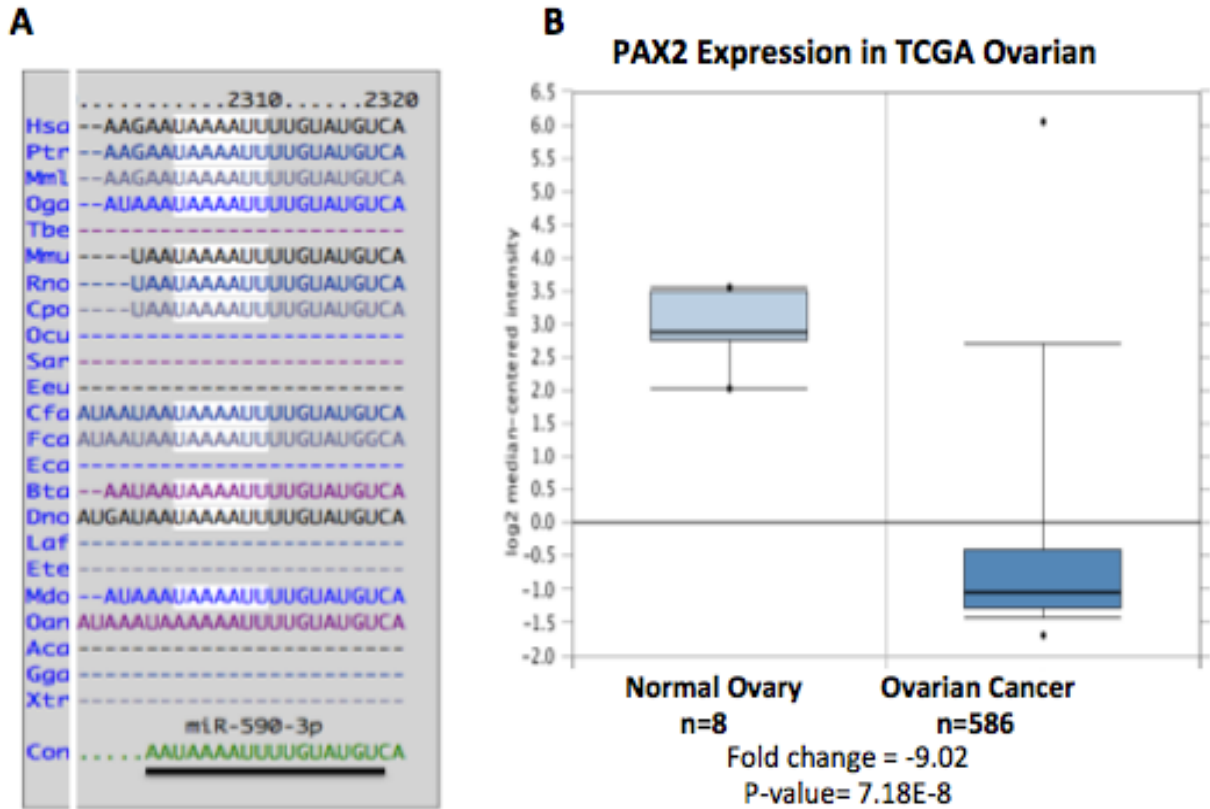


Figure 15: *In silico* analysis of *PAX2* as a potential downstream target of miR-590-3p. **A) MiR-590-3p binding region within *PAX2* 3'UTR is conservative among different species of mammals, including homosapiens (hsa), pan troglodytes (Ptr), macaca mulatta (mml), otolemur garnetti (oga), mus musculus (mmu), rattus norvegicus (rno), cavia porcellus (cpo), canis familiaris (cfa), felis catus (fca), bos Taurus (bta), dasypus novemcinctus (dno) and monodelphis domestica (mdo), obtained via TargetScan (Agarwal et al., 2015). **B**) Significant downregulation of *PAX2* in ovarian cancer (n=586) compared to normal ovarian tissues (n=8). The expression data was obtained from cancer genome atlas (TCGA) data portal through Oncomine database platform.**

Table 8: The alignment features of the putative miR-590-3p targets.

Predicted Target genes	Alignment	ΔG^* duplex	Accessibility **	A/U content ***	miRanda-mirSVR Score [§]	Prediction algorithm
SOX2	<pre> 3' ugaucgaauauguaUUUUAAu 5' hsa-miR-590-3p 606:5' aacgugaaaagaagAAAAUa 3' SOX2 </pre>	n/a	n/a	n/a	-0.3	miRanda
LEF1	<pre> 3' ugaUCGAAUAUGUAAUUUAAu 5' hsa-miR-590-3p 631:5' augAGCUUUUAAAUAUUUg 3' LEF1 </pre>	-1.9	6.46	0.78	-0.83	miRanda, Target scan, miR map
PAX2	<pre> 3' ugAUCGAAUAUGUAAUUUAAu 5' hsa-miR-590-3p : 2229:5' aaUAAUAAAGAAUUUUU 3' PAX2 </pre>	-3.6	7.19	0.85	-0.81	miRanda, Target scan, miR map

* Minimum Free Energy (MFE) of miRNA:mRNA duplex (should be minimal for optimal thermodynamic stability).

** Accessibility of the target site (energy required to unfold the mRNA 3'-UTR).

***A/U content around the seed (AU-rich 3'UTR is potentially less stable and more accessible).

§ mirSVR downregulation scores (good score ≤ -0.1).

3.8 The expression of the predicted target genes and its correlation with miR-590-3p in EOC tissues

To validate the targets of miR-590-3p, we examined the expression of the potential target genes in EOC tissues and analyzed the correlation between their levels and miR-590-3p levels. We categorized the EOC samples into two groups, the high miR-590-3p group that includes samples with elevated miR-590-3p more than two folds of that of the control and the low miR-590-3p group that encompasses the remaining samples. We examined the levels of *SOX2* at the mRNA and protein levels in representative samples from each group (Figure 16 A & B). Our results from examining six EOC samples at the RNA level and 14 EOC samples at the protein level showed no significant difference in *SOX2* levels between the two EOC groups (Figure 16C). Likewise, our results from examining *LEF1* mRNA levels in six representative EOC samples and *LEF1* protein levels in the 20 EOC samples appear to be not agreeing with our *in silico* results. Where the mRNA and the protein levels of *LEF1* were not significantly correlated with miR-590-3p (Figure 16 D, E &F).

PAX2 mRNA steady state levels were examined (Figure 7). And the levels of *PAX2* in EOC samples with elevated miR-590-3p were completely diminished. *PAX2* mRNA was only detected in EOC tissues with relatively lower miR-590-3p levels (Figure 18A). Negative correlation between *PAX2* and miR-590-3p levels was observed (Figure 18B). Nonetheless, further studies need to be conducted to validate *PAX2* as a regulatory target of miR-590-3p in EOC and to study the direct binding of miR-590-3p to *PAX2* 3'UTR.

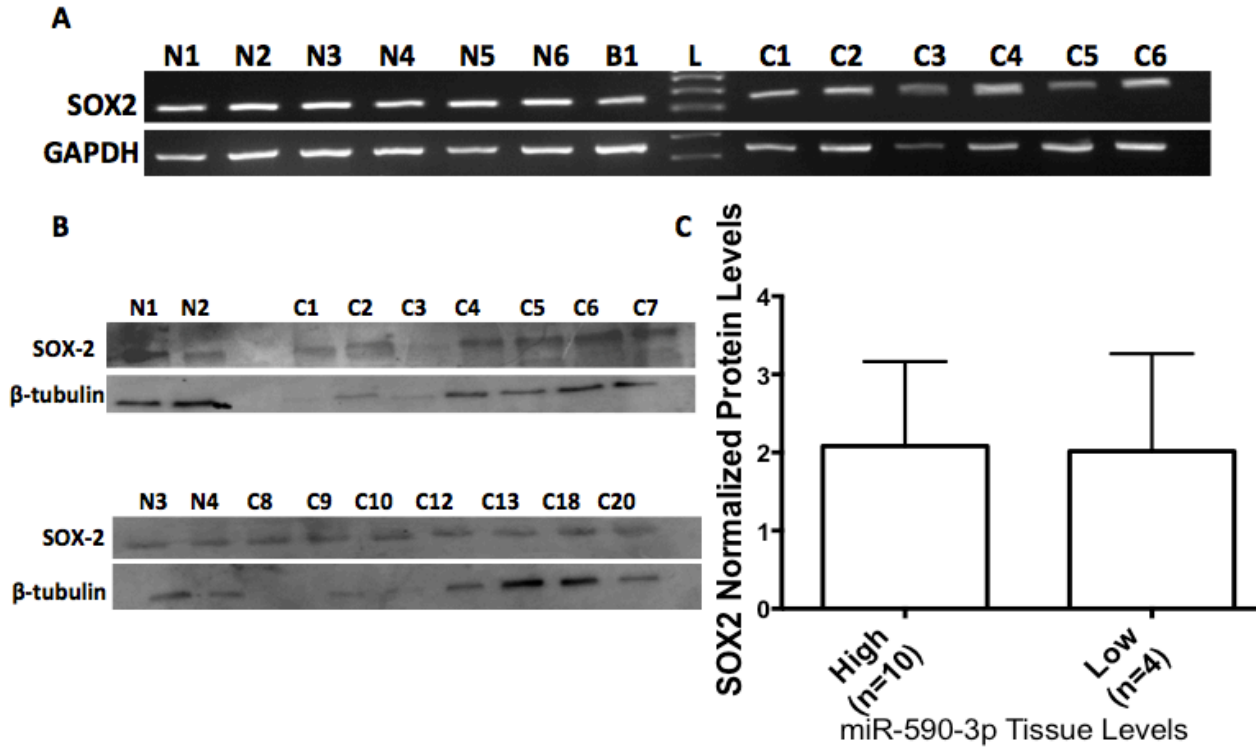
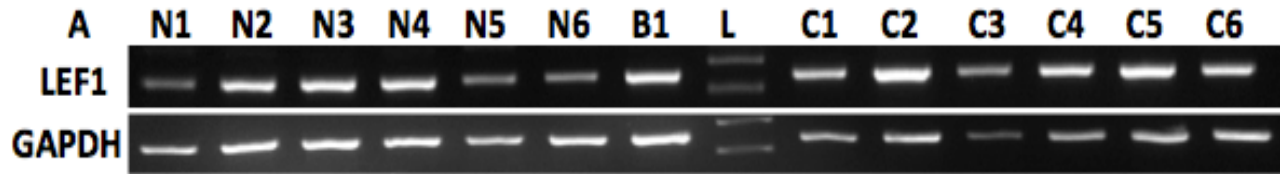
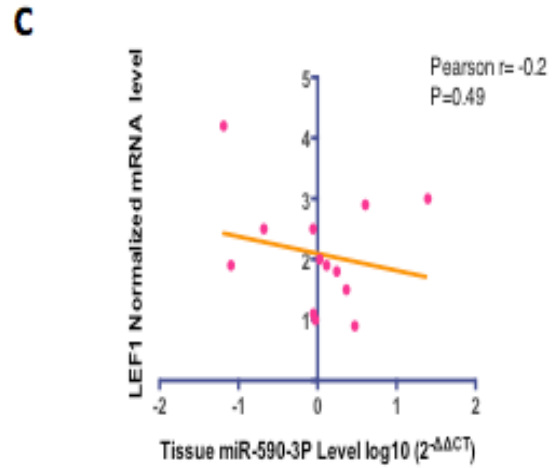
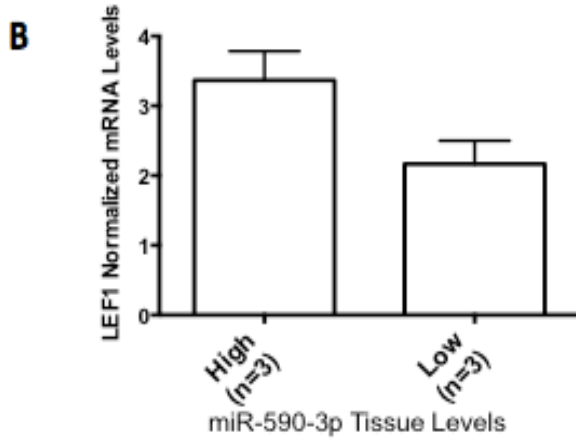


Figure 16: *SOX2* expression is not significantly correlated with miR-590-3p levels in EOC tissues. *SOX2* levels in EOC and control ovarian tissues were examined (A) at the RNA level using semi quantitative RT-PCR and (B) at the protein level using western blot. The loading control β -tubulin was not comparable in the examined samples. Therefore, bands intensities were analyzed using ImageJ and normalized to the loading control. C) The normalized *SOX2* protein levels did not significantly differ in EOC tumors with low levels of miR-590-3p (C1, C3, C5 & C20) and high miR-590-3p expressing EOC (C2, C4, C6, C7, C8, C9, C10, C12, C13, & C18).



Correlation of LEF1 levels with miR-590-3P expression



Correlation of LEF1 levels with miR-590-3P expression

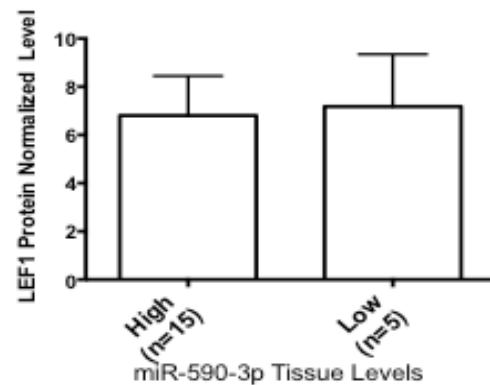
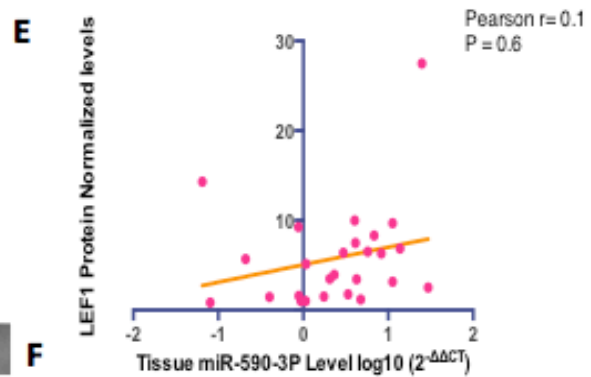
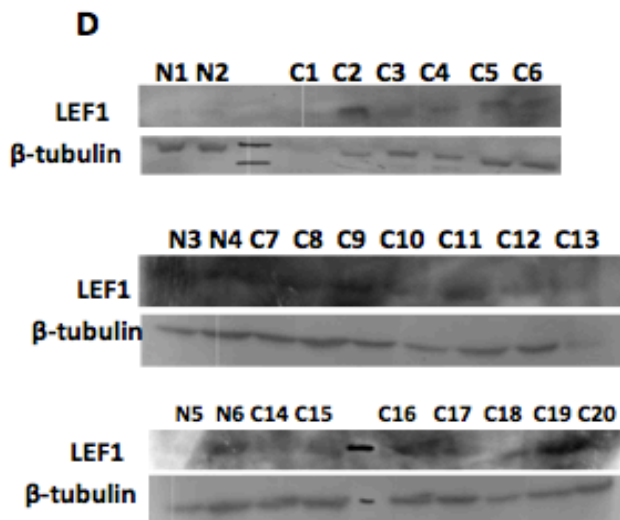


Figure 17: The correlation between *LEF1* expression and miR-590-3p in EOC. A) *LEF1* mRNA levels was assessed and B) its normalized levels did not significantly differ in EOC

tissues with lower miR-590-3p (C1, C3 & C5) or higher miR-590-3p levels (C2, C4 & C6). **C)** Also, no significant correlation was observed between *LEF1* mRNA and miR-590-3p levels. **D)** LEF1 protein levels were examined in EOC and control tissues. **E)** There was no significant correlation between the normalized LEF1 protein and miR-590-3p and **F)** there was no significant difference between LEF1 protein levels in EOC with high miR-590-3p levels and the EOC with relatively lower miR-590-3p levels (C1, C3, C5, C14 & C20)

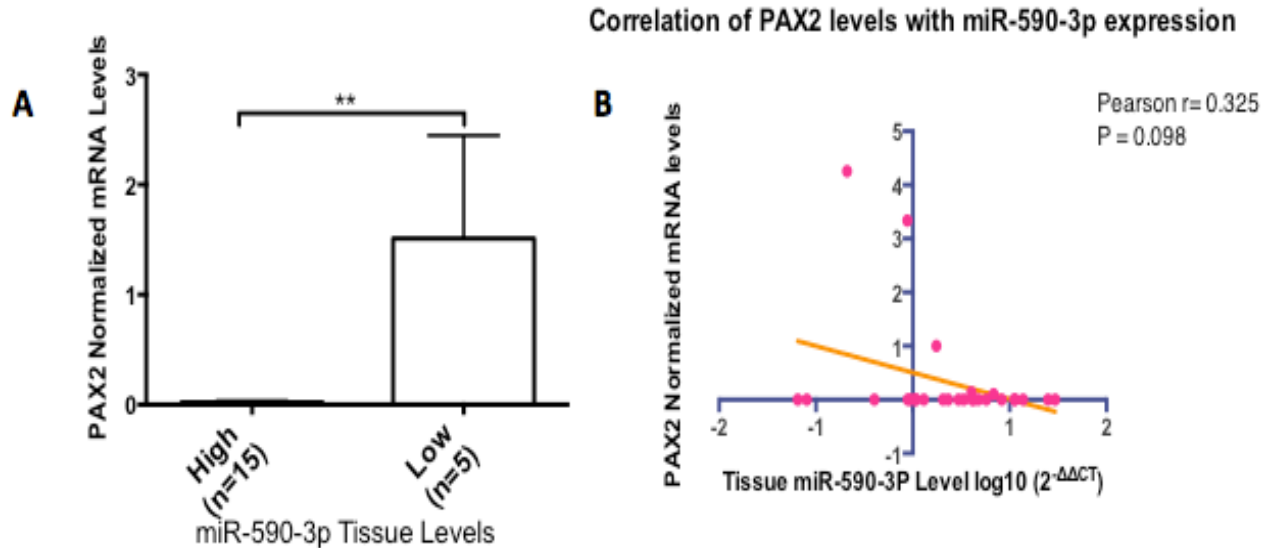


Figure 18: The correlation between the expression of *PAX2* and miR-590-3p. **A)** *PAX2* expression was associated with EOC samples with lower levels of miR-590-3p (C1, C3, C5, C14 and C20). **B)** Negative correlation between the normalized *PAX2* mRNA levels and miR-590-3p levels was observed. (**P<0.005)

3.9 MiR-590-3p expression profiles in different cancer types

Owing to the implied role of miR-590-3p in carcinogenesis, it was worth examining its expression pattern in other cancer types. Therefore, we utilized StarBase Pan-cancer analysis platform (http://starbase.sysu.edu.cn/pan_Cancer.php) (Li, Liu, Zhou, Qu, & Yang, 2014; Yang et al., 2011), which encompasses the expression profiles of miRNAs in 14 different cancer types that is available at The Cancer Genome Atlas (TCGA) Data Portal, to gain insight to the expression of miR-590-3p in various types of cancer. Interestingly, miR-590-3p showed inconsistent expression profiles among different cancer types. Nonetheless, there were no data fetched from StarBase Pan-cancer analysis platform about miR-590-3p in ovarian cancer. MiR-590-3p expression was significantly downregulated in papillary thyroid carcinoma with fold

change of 0.8 ($P=0.002$) (Figure 19). However, its levels showed to be upregulated in head and neck squamous cell carcinoma with fold change of 1.1 ($P=0.02$) (Figure 19).

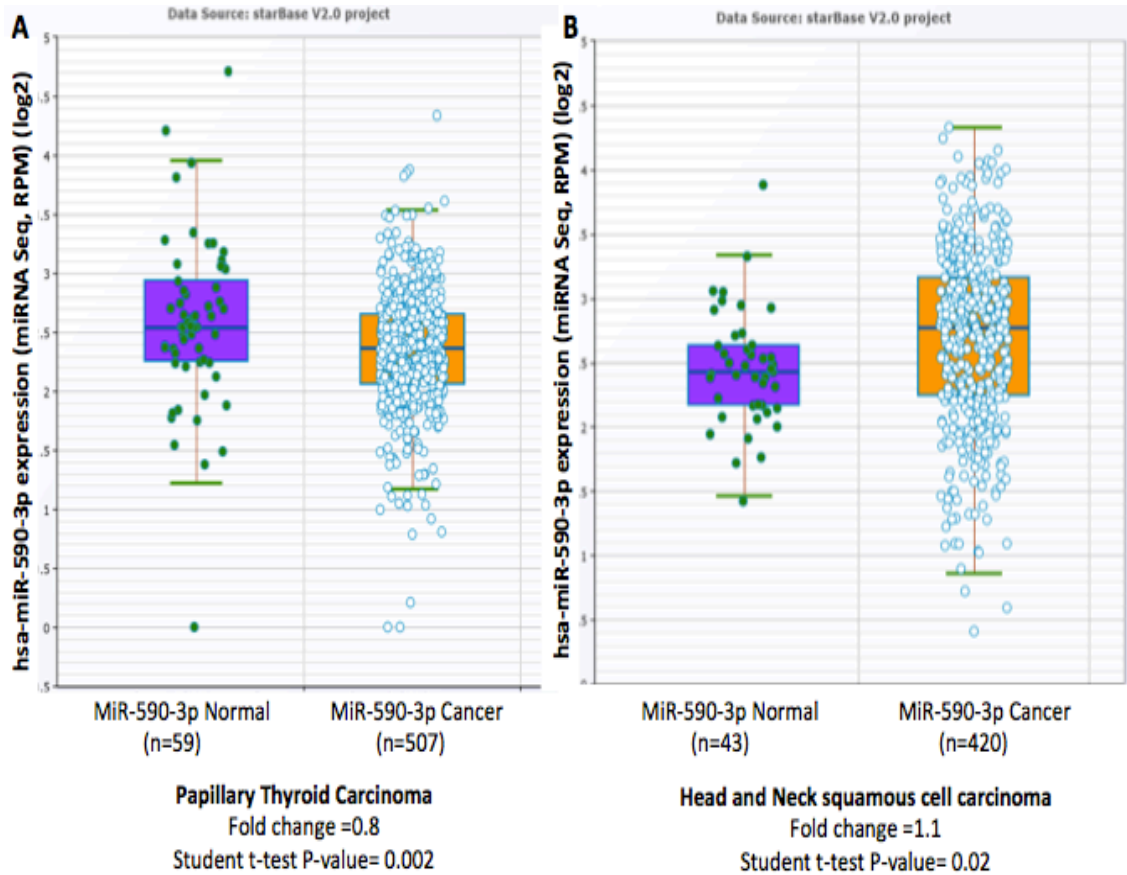


Figure 19: Expression profiles of miR-590-3p among different cancer types. MiR-590-3p showed different expression profiles among the 14 different cancer types analyzed using StarBase Pan-cancer analysis platform. For instance, **A)** miR-590-3p expression is significantly downregulated in papillary thyroid carcinoma samples ($P=0.002$). However, **B)** the levels of miR-590-3p is upregulated in head and neck squamous cell carcinoma ($P=0.02$). Data source is StarBase Pan-cancer analysis platform (http://starbase.sysu.edu.cn/pan_Cancer.php) (Li, Liu, Zhou, Qu, & Yang, 2014; Yang et al., 2011).

CHAPTER 4

Discussion, Conclusions and Future directions

EOC accounts for 90% of the ovarian malignancies, which is the most lethal gynecological cancer (Howlander N, 2015). The high mortality rate in ovarian cancer mainly stems from the late diagnosis at advanced stages. As, the five-year survival rate in the patients diagnosed at an advanced stage is only 21%; whereas the five-year survival rate is more than 90% of stage I ovarian cancer patients (Hoskins et al., 1992; Young et al., 1990). Although, the current diagnostic biomarker, CA125, can give an indication of the response to therapy, the disease progression and prognosis (Rustin et al., 1996), it has poor sensitivity especially for diagnosis of early-stage ovarian cancer (Havrilesky et al., 2008; Jacobs et al., 1993). Moreover, despite using a combination of biomarkers along with CA125 to increase its sensitivity in ovarian cancer diagnosis, survival rates did not improve significantly in the previous decades (Menon & Jacobs, 2000). Here, we observed similar results with the blood CA125 levels, where 15% of patients in the study showed normal levels of blood CA125, despite being diagnosed with ovarian cancer. Therefore, new effective diagnostic markers are needed for early diagnosis of ovarian cancer to reduce ovarian cancer mortality rate.

Circulating miRNAs are newly emerging potential diagnostic biomarkers. Being highly stable makes its measurement reproducible even after repeated freezing/thawing cycles or prolonged storage at room temperature. Several miRNAs showed to be differentially expressed in ovarian cancer, for instance miR-205, and let7 family. Nonetheless, similar expression patterns were observed in other cancer types, like let7-family that was downregulated in ovarian cancer as well as breast cancer. Also miR-205 was upregulated in ovarian cancer and it was also elevated in bladder and kidney cancer (Gottardo et al., 2007). On the other hand, miR-590-3p was found to be downregulated in bladder and kidney cancer, and to our knowledge, no work was done on miR-590-3p in ovarian cancer patients.

To study the expression pattern of miR-590-3p in EOC, serum samples from EOC patients, EOC tissues, as well as control serum and ovarian tissues were collected. The clinical stage of the tumor was assessed according to the International Federation of Gynecology and Obstetrics (FIGO), and the tumor grade was pathologically determined. However, tumor tissues encompass heterogeneous population with different levels of tumor cell differentiation, which make it

challenging to correlate the expression of a molecular marker with that of the tumor histopathological features. To overcome the intra-tumoral heterogeneity, we evaluated the histopathological characteristics of the surgical specimens at the molecular level through examining acknowledged molecular biomarkers using RT-PCR. Thus, a single RNA aliquot is being examined for histo-pathological biomarkers, as well as the levels of miR-590-3p. We examined the mRNA steady-state levels of *CA125/Mucin16* as a biomarker for ovarian cancer. We observed that the low levels of CA125 in blood reflected low expression levels of *CA125* in the tumor tissues. *CA125* levels were low in patients subjected to platinum-based combination chemotherapy, which is in agreement with prior studies that showed that CA125 levels reflect the ovarian carcinoma response to chemotherapy (Rustin et al., 1996). We used *CRP* as a biomarker for the clinical stage, and we observed elevated levels of *CRP* in advanced stages. *PAX2*, which is a biomarker for low-grade ovarian cancer, was only detected in low-grade EOC. Higher-grade EOC showed abolished expression of *PAX2*. In agreement with previous studies, *PAX2* expression was not detected in the ovarian mucinous carcinoma specimen (Schaner et al., 2003; Wang et al., 2015). Unexpectedly, we observed abolished *PAX2* expression in six low-grade ovarian serous carcinoma specimens. One possible explanation is the tissue heterogeneity and the different levels of cell differentiation within the samples.

In the present study, we found that circulating miR-590-3p in the serum is a promising diagnostic biomarker for EOC. As we showed that circulating miR-590-3p levels were elevated in EOC patients compared to healthy females (Figure 8). Moreover, elevated miR-590-3p was not observed in the patient with benign ovarian tumor. Serum miR-590-3p was elevated in both early and late stages (Figure 9). Remarkably, miR-590-3p was elevated in stage-IB EOC patient with low pre-operative levels of serum CA125 (10U/ml). Furthermore, the diagnostic ability of miR-590-3p to distinguish between stage-I patients and healthy controls showed 75% sensitivity at its optimal cutoff value, which is higher than the previously reported sensitivity of CA125 at early stages. As the sensitivity of CA125 to discriminate between stage I/II ovarian cancer patients (n=133) and healthy controls (n=396) was only 45.9% (Havrilesky et al., 2008). Therefore, our results suggest that miR-590-3p is a promising diagnostic biomarker for early diagnosis of EOC.

To study whether serum miR-590-3p reflects a dysregulation in EOC tissues, we examined the levels of miR-590-3p in the tumor tissues. Similarly, miR-590-3p was significantly upregulated in EOC relative to normal ovarian tissues (Figure 11). This observation is in accord with a

previous study that measured the ovarian cancer-derived exosomal miRNA content and its correlation with the ovarian tumor cellular miRNA and reported that the mature miR-590 was among the 175 miRNAs that exhibited equal levels in the tumor cells and the tumor-derived exosomes (Taylor et al., 2008). Our results suggest that the elevated serum miR-590-3p could be originated from the ovarian tumor cells, implying that it could be used for accurate diagnosis of ovarian cancer.

We observed a high correlation between tissue miR-590-3p and the tumor grade. As, miR-590-3p showed significant higher level in high-grade poorly-differentiated EOC relative to low-grade EOC (Figure 11). Its involvement in tumor cell differentiation is consistent with our bioinformatics analysis that predicted the role of miR-590-3p through analyzing the function of its down-stream target genes, which were significantly enriched in the cell differentiation processes. Similar expression pattern of miR-590-3p was previously reported in glioma that showed elevated levels of miR-590-3p in anaplastic gliomas and secondary glioblastomas relative to low-grade gliomas (Yan et al., 2014). The poorly differentiated EOC is usually associated with enhanced tumorigenic potential and aggressiveness (V. W. Chen et al., 2003; X. Chen et al., 2013; Vang et al., 2009). The elevated levels of miR-590-3p in poorly differentiated EOC urged us to examine the association of its levels with metastasis and EMT. Nonetheless, we were limited by the small sample size of cases with metastasis (n=3). Thus, there was no significant variation in miR-590-3p levels in the patients with metastasis and the EOC patients without metastasis. There is a current hypothesis that attempts to explain tumor progression, which suggest that tumor initiating cells can undergo epithelial to mesenchymal transition to reach a more advanced grade of differentiation (Heerboth et al., 2015). Therefore, EMT is crucial in ovarian cancer progression. This tumor progression does not necessarily imply that all the cells that underwent EMT will become metastatic (Sarkar et al., 2013). Therefore, we examined the mRNA steady-state levels of EMT-related markers, the epithelial marker E-cadherin, and the mesenchymal marker Vimentin, in EOC tissues to study the correlation between miR-590-3p and EMT in EOC. We observed that the mesenchymal marker Vimentin was elevated in EOC with high miR-590-3p levels relative to EOC tissues with relatively lower miR-590-3p and the control tissues (Figure 12). This observation indicates that miR-590-3p could be involved in the tumor progression and EMT.

The overexpression in EOC doesn't necessarily imply that miR-590-3p is playing an oncogenic role. Therefore, to clarify the role of miR-590-3p in EOC, we used bioinformatics analysis to predict the potential target genes of miR-590-3p and to study their expression profiles in ovarian cancer through analyzing the cancer genome atlas (TCGA) ovarian cancer gene expression data and microarray datasets retrieved from previous studies. We examined the levels of three potential downstream targets, *SOX2*, *LEF1* and *PAX2* in selected EOC samples that represent the high miR-590-3p EOC and the low miR-590-3p EOC, as well as the control group. Our *in silico* analysis of the TCGA ovarian cancer gene expression data showed that *SOX2* is downregulated in ovarian cancer relative to normal ovarian tissue (Figure 13). Nonetheless, *SOX2* steady-state levels in EOC tissues at the RNA and protein levels did not show significant correlation between *SOX2* and miR-590-3p levels (Figure 16). The negative correlation between *LEF1* and miR-590-3p expression that we observed from our *in silico* analysis of the ovarian cancer TCGA datasets using StarBase Pan-cancer analysis platform urged us to examine the levels of *LEF1* in EOC (Figure 14). This negative correlation was not observed in the studied EOC tissues at the RNA or the protein level (Figure 17). This could be owing to the different approaches used in quantifying the expression levels and also the heterogeneity of the tissue samples. Therefore, further studies need to be conducted on relatively larger sample size. Also using ovarian cancer cell lines could serve as a homogenous model of ovarian cancer that could be utilized to examine the effect of miR-590-3p ectopic expression or knockdown on the expression of its potential downstream target genes.

We observed that *PAX2* expression was completely abolished in EOC samples with high miR-590-3p levels, suggesting that it could be targeted by miR-590-3p (Figure 18). *PAX2* is a nuclear transcription factor, whose expression is essential in embryonic development, cellular differentiation, and organogenesis. Altered *PAX2* expression was observed in various cancer types, including ovarian cancer. Where, *PAX2* exhibits high expression in low-grade and low malignant potential ovarian serous carcinoma, but low level of gene expression in high-grade ovarian serous carcinoma (Tung et al., 2009). *PAX2* knockdown in *PAX2*-expressing ovarian cancer cell line (Tov21g malignant ovarian clear cell adenocarcinoma cell line) resulted in the reduction of cell proliferation and migration, suggesting an oncogenic role of *PAX2*. However, *PAX2* ectopic expression in ovarian serous adenocarcinoma cell lines (OVCA-432 and OVCAR)

resulted in a reduction in cell proliferation, suggesting that *PAX2* can act as an oncogene or tumor suppressor depending on the genetic basis of the tumor cells (Song et al., 2013).

The elevated levels of miR-590-3p in poorly-differentiated EOC, the negative correlation between miR-590-3p and *PAX2* expression, as well as the adoption of the EMT markers in the high miR-590-3p EOC, suggest that miR-590-3p could have a role in tumor development from healthy well-differentiated ovarian cell to dedifferentiate into poorly-differentiated tumor-initiating cells. Also, our results that miR-590-3p^{high}/*PAX2*^{low} signature is associated with poorly differentiated high-grade EOC could suggest another theory. Where the high-grade ovarian carcinoma with miR-590-3p^{high}/*PAX2*^{low} could have developed from different pathway or origin than that of the low-grade ovarian carcinoma. These hypothetical models require further investigation.

Moreover, through the analysis of the expression profiles of miRNAs available at The Cancer Genome Atlas (TCGA) Data Portal, we observed diverse expression patterns of miR-590-3p in different types of cancer (Figure 19). The discrepancy in miR-590-3p altered expression in cancer indicates that it could exhibit both tumor suppressor and oncogenic role depending on the genetic basis of the tumor cells that could be defined by the tumor origin and the stage of tumor progression. Therefore, more studies are still required to clarify the role of miR-590-3p in carcinogenesis. We were limited by not examining the levels of the potential downstream targets in all the samples and not examining the protein levels of *PAX2*. The direct binding of miR-590-3p to the 3'UTR of *PAX2* needs to be examined to confirm the direct regulation. We were also limited by the relatively small sample size. Also, further studies need to be conducted in cultured ovarian cancer cells to serve as a more homogenous model of ovarian cancer. As the tumor tissues comprise a highly heterogeneous population with different stages of tumor cell differentiation, which heighten the complexity in studying the role of miR-590-3p and its potential downstream targets in EOC carcinogenesis.

In conclusion, we have shown that circulating miR-590-3p is a promising diagnostic biomarker for early detection of epithelial ovarian cancer. Nonetheless, further studies need to be conducted on larger sample size. Our result of miR-590-3p levels in the serum is a step forward towards developing an approach for early-stage ovarian cancer detection. We showed that miR-590-3p was elevated in EOC tissues, with enhanced expression in high-grade poorly

differentiated tumors. The high miR-590-3p levels in EOC were associated with the adoption of EMT markers and abolished *PAX2* expression. The role of miRNAs expression in the progression of tumor initiating cells from normal well-differentiated cells is still unknown. The expression pattern of miR-590-3p in EOC tissues, as well as its *in silico* predicted downstream targets that were enriched in the cell differentiation processes, suggest that miR-590-3p could have a role in the tumor initiation stage.

References

- Agarwal, V., Bell, G. W., Nam, J. W., & Bartel, D. P. (2015). Predicting effective microRNA target sites in mammalian mRNAs. *Elife*, 4. doi:10.7554/eLife.05005
- Antolin, S., Calvo, L., Blanco-Calvo, M., Santiago, M., Lorenzo-Patino, M., Haz-Conde, M., Santamarina, I., Figueroa, A., Anton-Aparicio, L., & Valladares-Ayerbes, M. (2015). Circulating miR-200c and miR-141 and outcomes in patients with breast cancer. *BMC Cancer*, 15(1), 297. Retrieved from <http://www.biomedcentral.com/1471-2407/15/297>
- Bast, R. C., Hennessy, B., & Mills, G. B. (2009). The biology of ovarian cancer: new opportunities for translation. *Nat Rev Cancer*, 9(6), 415-428. Retrieved from <http://dx.doi.org/10.1038/nrc2644>
- Behm-Ansmant, I., Rehwinkel, J., Doerks, T., Stark, A., Bork, P., & Izaurralde, E. (2006). mRNA degradation by miRNAs and GW182 requires both CCR4:NOT deadenylase and DCP1:DCP2 decapping complexes. *Genes & Development*, 20(14), 1885-1898. doi:10.1101/gad.1424106
- Betel, D., Koppal, A., Agius, P., Sander, C., & Leslie, C. (2010). Comprehensive modeling of microRNA targets predicts functional non-conserved and non-canonical sites. *Genome Biology*, 11(8), R90. Retrieved from <http://genomebiology.com/2010/11/8/R90>
- Betel, D., Wilson, M., Gabow, A., Marks, D. S., & Sander, C. (2008). The microRNA.org resource: targets and expression. *Nucleic Acids Research*, 36(suppl 1), D149-D153. doi:10.1093/nar/gkm995
- Bonome, T., Levine, D. A., Shih, J., Randonovich, M., Pise-Masison, C. A., Bogomolny, F., Ozbun, L., Brady, J., Barrett, J. C., Boyd, J., & Birrer, M. J. (2008). A Gene Signature Predicting for Survival in Suboptimally Debulked Patients with Ovarian Cancer. *Cancer Research*, 68(13), 5478-5486. doi:10.1158/0008-5472.can-07-6595
- Borchert, G. M., Lanier, W., & Davidson, B. L. (2006). RNA polymerase III transcribes human microRNAs. *Nat Struct Mol Biol*, 13(12), 1097-1101. doi:http://www.nature.com/nsmb/journal/v13/n12/suppinfo/nsmb1167_S1.html
- Caraguel, C. G. B., Stryhn, H., Gagné, N., Dohoo, I. R., & Hammell, K. L. (2011). Selection of a Cutoff Value for Real-Time Polymerase Chain Reaction Results to Fit a Diagnostic Purpose: Analytical and Epidemiologic Approaches. *Journal of Veterinary Diagnostic Investigation*, 23(1), 2-15. doi:10.1177/104063871102300102
- Chen, V. W., Ruiz, B., Killeen, J. L., Coté, T. R., Wu, X. C., Correa, C. N., & Howe, H. L. (2003). Pathology and classification of ovarian tumors. *Cancer*, 97(S10), 2631-2642. doi:10.1002/cncr.11345
- Chen, X., Zhang, J., Zhang, Z., Li, H., Cheng, W., & Liu, J. (2013). Cancer stem cells, epithelial-mesenchymal transition, and drug resistance in high-grade ovarian serous carcinoma. *Human Pathology*, 44(11), 2373-2384. doi:<http://dx.doi.org/10.1016/j.humpath.2013.05.001>

- Dhayat, S. A., Hüsing, A., Senninger, N., Schmidt, H. H., Haier, J., Wolters, H., & Kabar, I. (2015). Circulating microRNA-200 Family as Diagnostic Marker in Hepatocellular Carcinoma. *PLoS One*, *10*(10), e0140066. doi:10.1371/journal.pone.0140066
- Dubeau, L. (2008). The cell of origin of ovarian epithelial tumours. *The Lancet Oncology*, *9*(12), 1191-1197. doi:[http://dx.doi.org/10.1016/S1470-2045\(08\)70308-5](http://dx.doi.org/10.1016/S1470-2045(08)70308-5)
- El-Hefnawy, T., Raja, S., Kelly, L., Bigbee, W. L., Kirkwood, J. M., Luketich, J. D., & Godfrey, T. E. (2004). Characterization of Amplifiable, Circulating RNA in Plasma and Its Potential as a Tool for Cancer Diagnostics. *Clinical Chemistry*, *50*(3), 564-573. doi:10.1373/clinchem.2003.028506
- Eulalio, A., Mano, M., Ferro, M. D., Zentilin, L., Sinagra, G., Zacchigna, S., & Giacca, M. (2012). Functional screening identifies miRNAs inducing cardiac regeneration. *Nature*, *492*(7429), 376-381. doi:<http://www.nature.com/nature/journal/v492/n7429/abs/nature11739.html-supplementary-information>
- Février, B., & Raposo, G. (2004). Exosomes: endosomal-derived vesicles shipping extracellular messages. *Current Opinion in Cell Biology*, *16*(4), 415-421. doi:<http://dx.doi.org/10.1016/j.ceb.2004.06.003>
- Fidler, I., & Hart, I. (1982). Biological diversity in metastatic neoplasms: origins and implications. *Science*, *217*(4564), 998-1003. doi:10.1126/science.7112116
- Gadducci, A., Cosio, S., Tana, R., & Genazzani, A. R. (2009). Serum and tissue biomarkers as predictive and prognostic variables in epithelial ovarian cancer. *Critical reviews in oncology/hematology*, *69*(1), 12-27.
- Gang, Y., Stefanie, B., & Chun, P. (2012). Etiology and overview *Advances in Ovarian Cancer Management* (pp. 6-16): Future Medicine Ltd.
- Gao, Y.-c., & Wu, J. (2015). MicroRNA-200c and microRNA-141 as potential diagnostic and prognostic biomarkers for ovarian cancer. *Tumor Biology*, *36*(6), 4843-4850. doi:10.1007/s13277-015-3138-3
- Gottardo, F., Liu, C. G., Ferracin, M., Calin, G. A., Fassan, M., Bassi, P., Sevignani, C., Byrne, D., Negrini, M., Pagano, F., Gomella, L. G., Croce, C. M., & Baffa, R. (2007). Micro-RNA profiling in kidney and bladder cancers. *Urologic Oncology: Seminars and Original Investigations*, *25*(5), 387-392. doi:<http://dx.doi.org/10.1016/j.urolonc.2007.01.019>
- Gregory, R. I., Yan, K.-p., Amuthan, G., Chendrimada, T., Doratotaj, B., Cooch, N., & Shiekhattar, R. (2004). The Microprocessor complex mediates the genesis of microRNAs. *Nature*, *432*(7014), 235-240. doi:http://www.nature.com/nature/journal/v432/n7014/supinfo/nature03120_S1.html
- Guo, F., Tian, J., Lin, Y., Jin, Y., Wang, L., & Cui, M. (2013). Serum microRNA-92 expression in patients with ovarian epithelial carcinoma. *Journal of International Medical Research*, *41*(5), 1456-1461. doi:10.1177/0300060513487652

- Havrilesky, L. J., Whitehead, C. M., Rubatt, J. M., Cheek, R. L., Groelke, J., He, Q., Malinowski, D. P., Fischer, T. J., & Berchuck, A. (2008). Evaluation of biomarker panels for early stage ovarian cancer detection and monitoring for disease recurrence. *Gynecologic Oncology*, *110*(3), 374-382. doi:<http://dx.doi.org/10.1016/j.ygyno.2008.04.041>
- Heerboth, S., Housman, G., Leary, M., Longacre, M., Byler, S., Lapinska, K., Willbanks, A., & Sarkar, S. (2015). EMT and tumor metastasis. *Clinical and Translational Medicine*, *4*, 6. doi:10.1186/s40169-015-0048-3
- Hefler-Frischmuth, K., Hefler, L. A., Heinze, G., Paseka, V., Grimm, C., & Tempfer, C. B. (2009). Serum C-reactive protein in the differential diagnosis of ovarian masses. *European Journal of Obstetrics & Gynecology and Reproductive Biology*, *147*(1), 65-68. doi:<http://dx.doi.org/10.1016/j.ejogrb.2009.06.010>
- Heintz, A. P. M., Odicino, F., Maisonneuve, P., Quinn, M. A., Benedet, J. L., Creasman, W. T., Ngan, H. Y. S., Pecorelli, S., & Beller, U. (2006). Carcinoma of the Ovary. *International Journal of Gynecology & Obstetrics*, *95*, Supplement 1, S161-S192. doi:[http://dx.doi.org/10.1016/S0020-7292\(06\)60033-7](http://dx.doi.org/10.1016/S0020-7292(06)60033-7)
- Høgdall, E. V. S., Christensen, L., Kjaer, S. K., Blaakaer, J., Kjærbye-Thygesen, A., Gayther, S., Jacobs, I. J., & Høgdall, C. K. (2007). CA125 expression pattern, prognosis and correlation with serum CA125 in ovarian tumor patients: From The Danish "MALOVA" Ovarian Cancer Study. *Gynecologic Oncology*, *104*(3), 508-515. doi:<http://dx.doi.org/10.1016/j.ygyno.2006.09.028>
- Hong, F., Li, Y., Xu, Y., & Zhu, L. (2013). Prognostic significance of serum microRNA-221 expression in human epithelial ovarian cancer. *Journal of International Medical Research*, *41*(1), 64-71. doi:10.1177/0300060513475759
- Hoskins, W. J., Bundy, B. N., Thigpen, J. T., & Omura, G. A. (1992). The influence of cytoreductive surgery on recurrence-free interval and survival in small-volume Stage III epithelial ovarian cancer: A gynecologic oncology group study. *Gynecologic Oncology*, *47*(2), 159-166. doi:[http://dx.doi.org/10.1016/0090-8258\(92\)90100-W](http://dx.doi.org/10.1016/0090-8258(92)90100-W)
- Howlader N, N. A., Krapcho M, Garshell J, Miller D, Altekruse SF, Kosary CL, Yu M, Ruhl J, Tatalovich Z, Mariotto A, Lewis DR, Chen HS, Feuer EJ, Cronin KA (2015). SEER Cancer Statistics Review, 1975-2012, National Cancer Institute. Retrieved from http://seer.cancer.gov/csr/1975_2012/.
- Hunter, M. P., Ismail, N., Zhang, X., Aguda, B. D., Lee, E. J., Yu, L., Xiao, T., Schafer, J., Lee, M.-L. T., Schmittgen, T. D., Nana-Sinkam, S. P., Jarjoura, D., & Marsh, C. B. (2008). Detection of microRNA Expression in Human Peripheral Blood Microvesicles. *PLoS One*, *3*(11), e3694. doi:10.1371/journal.pone.0003694
- Hutvagner, G., McLachlan, J., Pasquinelli, A. E., Bálint, É., Tuschl, T., & Zamore, P. D. (2001). A Cellular Function for the RNA-Interference Enzyme Dicer in the Maturation of the let-7 Small Temporal RNA. *Science*, *293*(5531), 834-838. doi:10.1126/science.1062961
- Hutvagner, G., & Zamore, P. D. (2002). A microRNA in a Multiple-Turnover RNAi Enzyme Complex. *Science*, *297*(5589), 2056-2060. doi:10.1126/science.1073827

- Jacobs, I., Davies, A. P., Bridges, J., Stabile, I., Fay, T., Lower, A., Grudzinskas, J. G., & Oram, D. (1993). Prevalence screening for ovarian cancer in postmenopausal women by CA 125 measurement and ultrasonography. *BMJ*, *306*(6884), 1030-1034. doi:10.1136/bmj.306.6884.1030
- Jemal, A., Bray, F., Center, M. M., Ferlay, J., Ward, E., & Forman, D. (2011). Global cancer statistics. *CA: A Cancer Journal for Clinicians*, *61*(2), 69-90. doi:10.3322/caac.20107
- John, B., Enright, A. J., Aravin, A., Tuschl, T., Sander, C., & Marks, D. S. (2004). Human MicroRNA targets. *PLoS Biol*, *2*(11), e363. doi:10.1371/journal.pbio.0020363
- Kan, C. W., Hahn, M., Gard, G., Maidens, J., Huh, J. Y., Marsh, D., & Howell, V. (2012). Elevated levels of circulating microRNA-200 family members correlate with serous epithelial ovarian cancer. *BMC Cancer*, *12*(1), 627. Retrieved from <http://www.biomedcentral.com/1471-2407/12/627>
- Kosaka, N., Izumi, H., Sekine, K., & Ochiya, T. (2010). microRNA as a new immune-regulatory agent in breast milk. *Silence*, *1*, 7-7. doi:10.1186/1758-907X-1-7
- Kuhlmann, J. D., Baraniskin, A., Hahn, S. A., Mosel, F., Bredemeier, M., Wimberger, P., Kimmig, R., & Kasimir-Bauer, S. (2014). Circulating U2 Small Nuclear RNA Fragments as a Novel Diagnostic Tool for Patients with Epithelial Ovarian Cancer. *Clinical Chemistry*, *60*(1), 206-213. doi:10.1373/clinchem.2013.213066
- Ławicki, S., Będkowska, G. E., Gacuta-Szumarska, E., & Szmitkowski, M. (2013). The plasma concentration of VEGF, HE4 and CA125 as a new biomarkers panel in different stages and sub-types of epithelial ovarian tumors. *Journal of Ovarian Research*, *6*(1), 1-11. doi:10.1186/1757-2215-6-45
- Lee, S., Yu, K.-R., Ryu, Y.-S., Oh, Y., Hong, I.-S., Kim, H.-S., Lee, J., Kim, S., Seo, K.-W., & Kang, K.-S. (2014). miR-543 and miR-590-3p regulate human mesenchymal stem cell aging via direct targeting of AIMP3/p18. *AGE*, *36*(6), 1-17. doi:10.1007/s11357-014-9724-2
- Lee, Y., Jeon, K., Lee, J. T., Kim, S., & Kim, V. N. (2002). MicroRNA maturation: stepwise processing and subcellular localization. *The EMBO Journal*, *21*(17), 4663-4670. doi:10.1093/emboj/cdf476
- Lee, Y., Kim, M., Han, J., Yeom, K.-H., Lee, S., Baek, S. H., & Kim, V. N. (2004). MicroRNA genes are transcribed by RNA polymerase II. *The EMBO Journal*, *23*(20), 4051-4060. doi:10.1038/sj.emboj.7600385
- Li, J.-H., Liu, S., Zhou, H., Qu, L.-H., & Yang, J.-H. (2014). starBase v2.0: decoding miRNA-ncRNA, miRNA-ncRNA and protein-RNA interaction networks from large-scale CLIP-Seq data. *Nucleic Acids Research*, *42*(D1), D92-D97. doi:10.1093/nar/gkt1248
- Liang, H., Jiang, Z., Xie, G., & Lu, Y. (2015). Serum microRNA-145 as a novel biomarker in human ovarian cancer. *Tumor Biology*, *36*(7), 5305-5313. doi:10.1007/s13277-015-3191-y
- Liu, Q., Wang, G., Chen, Y., Li, G., Yang, D., & Kang, J. (2014). A miR-590/Acvr2a/Rad51b Axis Regulates DNA Damage Repair during mESC Proliferation. *Stem Cell Reports*, *3*(6), 1103-1117. doi:<http://dx.doi.org/10.1016/j.stemcr.2014.10.006>

- Livak, K. J., & Schmittgen, T. D. (2001). Analysis of Relative Gene Expression Data Using Real-Time Quantitative PCR and the 2- $\Delta\Delta$ CT Method. *Methods*, 25(4), 402-408. doi:<http://dx.doi.org/10.1006/meth.2001.1262>
- Menon, U., & Jacobs, I. J. (2000). Recent developments in ovarian cancer screening. *Current Opinion in Obstetrics and Gynecology*, 12(1), 39-42. Retrieved from http://journals.lww.com/co-obgyn/Fulltext/2000/02000/Recent_developments_in_ovarian_cancer_screening.7.aspx
- Mitchell, P. S., Parkin, R. K., Kroh, E. M., Fritz, B. R., Wyman, S. K., Pogosova-Agadjanyan, E. L., Peterson, A., Noteboom, J., O'Briant, K. C., Allen, A., Lin, D. W., Urban, N., Drescher, C. W., Knudsen, B. S., Stirewalt, D. L., Gentleman, R., Vessella, R. L., Nelson, P. S., Martin, D. B., & Tewari, M. (2008). Circulating microRNAs as stable blood-based markers for cancer detection. *Proceedings of the National Academy of Sciences*, 105(30), 10513-10518. doi:10.1073/pnas.0804549105
- Mo, M., Peng, F., Wang, L. U., Peng, L., Lan, G., & Yu, S. (2013). Roles of mitochondrial transcription factor A and microRNA-590-3p in the development of bladder cancer. *Oncology letters*, 6(2), 617-623. doi:10.3892/ol.2013.1419
- Nottrott, S., Simard, M. J., & Richter, J. D. (2006). Human let-7a miRNA blocks protein production on actively translating polyribosomes. *Nat Struct Mol Biol*, 13(12), 1108-1114. Retrieved from <http://dx.doi.org/10.1038/nsmb1173>
- Pang, H., Zheng, Y., Zhao, Y., Xiu, X., & Wang, J. (2015). miR-590-3p suppresses cancer cell migration, invasion and epithelial-mesenchymal transition in glioblastoma multiforme by targeting ZEB1 and ZEB2. *Biochemical and Biophysical Research Communications*. doi:<http://dx.doi.org/10.1016/j.bbrc.2015.11.025>
- Petersen, C. P., Bordeleau, M.-E., Pelletier, J., & Sharp, P. A. (2006). Short RNAs Repress Translation after Initiation in Mammalian Cells. *Molecular Cell*, 21(4), 533-542. doi:<http://dx.doi.org/10.1016/j.molcel.2006.01.031>
- Pigati, L., Yaddanapudi, S. C. S., Iyengar, R., Kim, D.-J., Hearn, S. A., Danforth, D., Hastings, M. L., & Duelli, D. M. (2010). Selective Release of MicroRNA Species from Normal and Malignant Mammary Epithelial Cells. *PLoS One*, 5(10), e13515. doi:10.1371/journal.pone.0013515
- Resnick, K. E., Alder, H., Hagan, J. P., Richardson, D. L., Croce, C. M., & Cohn, D. E. (2009). The detection of differentially expressed microRNAs from the serum of ovarian cancer patients using a novel real-time PCR platform. *Gynecologic Oncology*, 112(1), 55-59. doi:<http://dx.doi.org/10.1016/j.ygyno.2008.08.036>
- Rhodes, D. R., Yu, J., Shanker, K., Deshpande, N., Varambally, R., Ghosh, D., Barrette, T., Pandey, A., & Chinnaiyan, A. M. (2004). ONCOMINE: a cancer microarray database and integrated data-mining platform. *Neoplasia*, 6(1), 1-6. Retrieved from <http://www.ncbi.nlm.nih.gov/pubmed/15068665>
- Rosen, D. G., Wang, L., Atkinson, J. N., Yu, Y., Lu, K. H., Diamandis, E. P., Hellstrom, I., Mok, S. C., Liu, J., & Bast Jr, R. C. (2005). Potential markers that complement expression of

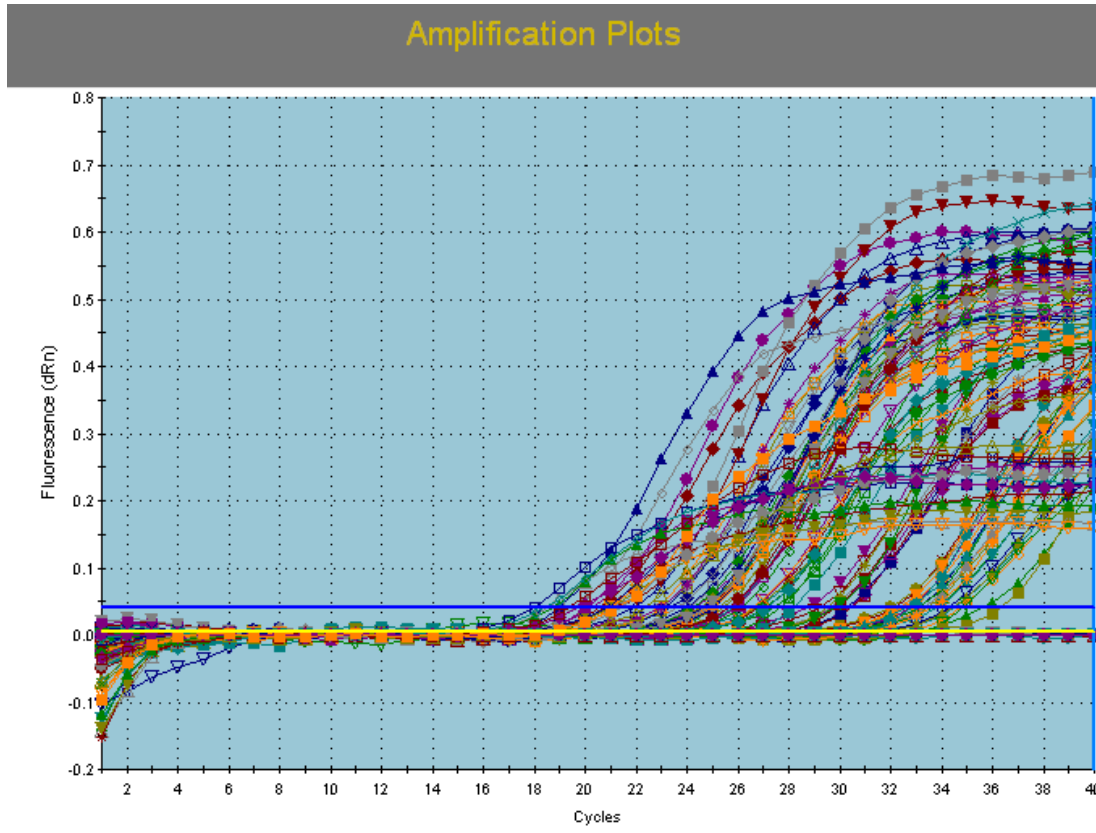
- CA125 in epithelial ovarian cancer. *Gynecologic Oncology*, 99(2), 267-277.
doi:<http://dx.doi.org/10.1016/j.ygyno.2005.06.040>
- Rustin, G. J., Nelstrop, A. E., McClean, P., Brady, M. F., McGuire, W. P., Hoskins, W. J., Mitchell, H., & Lambert, H. E. (1996). Defining response of ovarian carcinoma to initial chemotherapy according to serum CA 125. *Journal of Clinical Oncology*, 14(5), 1545-1551. Retrieved from <http://jco.ascopubs.org/content/14/5/1545.abstract>
- Sankaranarayanan, R., & Ferlay, J. Worldwide burden of gynaecological cancer: The size of the problem. *Best Practice & Research Clinical Obstetrics & Gynaecology*, 20(2), 207-225. doi:10.1016/j.bpobgyn.2005.10.007
- Sarkar, S., Horn, G., Moulton, K., Oza, A., Byler, S., Kokolus, S., & Longacre, M. (2013). Cancer Development, Progression, and Therapy: An Epigenetic Overview. *International Journal of Molecular Sciences*, 14(10), 21087-21113. doi:10.3390/ijms141021087
- Schaner, M. E., Ross, D. T., Ciaravino, G., Sørli, T., Troyanskaya, O., Diehn, M., Wang, Y. C., Duran, G. E., Sikic, T. L., Caldeira, S., Skomedal, H., Tu, I. P., Hernandez-Boussard, T., Johnson, S. W., O'Dwyer, P. J., Fero, M. J., Kristensen, G. B., Børresen-Dale, A.-L., Hastie, T., Tibshirani, R., van de Rijn, M., Teng, N. N., Longacre, T. A., Botstein, D., Brown, P. O., & Sikic, B. I. (2003). Gene Expression Patterns in Ovarian Carcinomas. *Molecular Biology of the Cell*, 14(11), 4376-4386. doi:10.1091/mbc.E03-05-0279
- Shapira, I., Oswald, M., Lovecchio, J., Khalili, H., Menzin, A., Whyte, J., Dos Santos, L., Liang, S., Bhuiya, T., Keogh, M., Mason, C., Sultan, K., Budman, D., Gregersen, P. K., & Lee, A. T. (2014). Circulating biomarkers for detection of ovarian cancer and predicting cancer outcomes. *Br J Cancer*, 110(4), 976-983. doi:10.1038/bjc.2013.795
- Song, H., Kwan, S.-Y., Izaguirre, D. I., Zu, Z., Tsang, Y. T., Tung, C. S., King, E. R., Mok, S. C., Gershenson, D. M., & Wong, K.-K. (2013). PAX2 Expression in Ovarian Cancer. *International Journal of Molecular Sciences*, 14(3), 6090-6105. doi:10.3390/ijms14036090
- Taylor, D. D., & Gercel-Taylor, C. (2008). MicroRNA signatures of tumor-derived exosomes as diagnostic biomarkers of ovarian cancer. *Gynecologic Oncology*, 110(1), 13-21. doi:<http://dx.doi.org/10.1016/j.ygyno.2008.04.033>
- Thomson, J. M., Newman, M., Parker, J. S., Morin-Kensicki, E. M., Wright, T., & Hammond, S. M. (2006). Extensive post-transcriptional regulation of microRNAs and its implications for cancer. *Genes & Development*, 20(16), 2202-2207. doi:10.1101/gad.1444406
- Toiyama, Y., Hur, K., Tanaka, K., Inoue, Y., Kusunoki, M., Boland, C. R., & Goel, A. (2014). Serum miR-200c is a novel prognostic and metastasis-predictive biomarker in patients with colorectal cancer. *Annals of surgery*, 259(4), 735-743. doi:10.1097/SLA.0b013e3182a6909d
- Tung, C. S., Mok, S. C., Tsang, Y. T. M., Zu, Z., Song, H., Liu, J., Deavers, M. T., Malpica, A., Wolf, J. K., Lu, K. H., Gershenson, D. M., & Wong, K.-K. (2009). PAX2 expression in low malignant potential ovarian tumors and low-grade ovarian serous carcinomas. *Mod Pathol*, 22(9), 1243-1250.

doi:<http://www.nature.com/modpathol/journal/v22/n9/suppinfo/modpathol200992s1.html>

- Ulitsky, I., Laurent, L. C., & Shamir, R. (2010). Towards computational prediction of microRNA function and activity. *Nucleic Acids Res*, *38*(15), e160. doi:10.1093/nar/gkq570
- Valadi, H., Ekstrom, K., Bossios, A., Sjostrand, M., Lee, J. J., & Lotvall, J. O. (2007). Exosome-mediated transfer of mRNAs and microRNAs is a novel mechanism of genetic exchange between cells. *Nat Cell Biol*, *9*(6), 654-659. doi:http://www.nature.com/ncb/journal/v9/n6/suppinfo/ncb1596_S1.html
- Valladares-Ayerbes, M., Reboredo, M., Medina-Villaamil, V., Iglesias-Diaz, P., Lorenzo-Patino, M., Haz, M., Santamarina, I., Blanco, M., Fernandez-Tajes, J., Quindos, M., Carral, A., Figueroa, A., Anton-Aparicio, L., & Calvo, L. (2012). Circulating miR-200c as a diagnostic and prognostic biomarker for gastric cancer. *Journal of Translational Medicine*, *10*(1), 186. Retrieved from <http://www.translational-medicine.com/content/10/1/186>
- Vang, R., Shih, I.-M., & Kurman, R. J. (2009). OVARIAN LOW-GRADE AND HIGH-GRADE SEROUS CARCINOMA: Pathogenesis, Clinicopathologic and Molecular Biologic Features, and Diagnostic Problems. *Advances in anatomic pathology*, *16*(5), 267-282. doi:10.1097/PAP.0b013e3181b4fffa
- Wang, M., Ma, H., Pan, Y., Xiao, W., Li, J., Yu, J., & He, J. (2015). PAX2 and PAX8 Reliably Distinguishes Ovarian Serous Tumors From Mucinous Tumors. *Applied Immunohistochemistry & Molecular Morphology*, *23*(4), 280-287. doi:10.1097/pai.0000000000000065
- Weber, J. A., Baxter, D. H., Zhang, S., Huang, D. Y., How Huang, K., Jen Lee, M., Galas, D. J., & Wang, K. (2010). The MicroRNA Spectrum in 12 Body Fluids. *Clinical Chemistry*, *56*(11), 1733-1741. doi:10.1373/clinchem.2010.147405
- Wu, L., Fan, J., & Belasco, J. G. (2006). MicroRNAs direct rapid deadenylation of mRNA. *Proceedings of the National Academy of Sciences of the United States of America*, *103*(11), 4034-4039. doi:10.1073/pnas.0510928103
- Xiaohui, X., Jun, L., Kulbokas, E. J., Todd, R. G., Vamsi, M., Kerstin, L.-T., Eric, S. L., & Manolis, K. (2005). Systematic discovery of regulatory motifs in human promoters and 3' UTRs by comparison of several mammals. *Nature*, *434*(7031), 338-345. doi:10.1038/nature03441
- Yan, W., Li, R., Liu, Y., Yang, P., Wang, Z., Zhang, C., Bao, Z., Zhang, W., You, Y., & Jiang, T. (2014). MicroRNA expression patterns in the malignant progression of gliomas and a 5-microRNA signature for prognosis. *Oncotarget*, *5*(24), 12908-12915.
- Yang, H., Zheng, W., Zhao, W., Guan, C., & An, J. (2013). [Roles of miR-590-5p and miR-590-3p in the development of hepatocellular carcinoma]. *Nan fang yi ke da xue xue bao= Journal of Southern Medical University*, *33*(6), 804-811.
- Yang, J.-H., Li, J.-H., Shao, P., Zhou, H., Chen, Y.-Q., & Qu, L.-H. (2011). starBase: a database for exploring microRNA-mRNA interaction maps from Argonaute CLIP-Seq and

- Degradome-Seq data. *Nucleic Acids Research*, 39(suppl 1), D202-D209.
doi:10.1093/nar/gkq1056
- Young, R. C., Walton, L. A., Ellenberg, S. S., Homesley, H. D., Wilbanks, G. D., Decker, D. G., Miller, A., Park, R., & Major, F. (1990). Adjuvant Therapy in Stage I and Stage II Epithelial Ovarian Cancer. *New England Journal of Medicine*, 322(15), 1021-1027.
doi:doi:10.1056/NEJM199004123221501
- Yun-Zhao Xu1, Q.-H. X., Wen-Liang Ge2, Xiao-Qian Zhang1. (2013). Identification of Serum MicroRNA-21 as a Biomarker for Early Detection and Prognosis in Human Epithelial Ovarian Cancer. *Asian Pacific Journal of Cancer Prevention*, 14, 4.
doi:<http://dx.doi.org/10.7314/APJCP.2013.14.2.1057>
- Zernecke, A., Bidzhekov, K., Noels, H., Shagdarsuren, E., Gan, L., Denecke, B., Hristov, M., Köppel, T., Jahantigh, M. N., Lutgens, E., Wang, S., Olson, E. N., Schober, A., & Weber, C. (2009). Delivery of MicroRNA-126 by Apoptotic Bodies Induces CXCL12-Dependent Vascular Protection. *Science Signaling*, 2(100), ra81-ra81.
doi:10.1126/scisignal.2000610
- Zhang, Q., Kandic, I., Faughnan, M. E., & Kutryk, M. J. (2013). Elevated circulating microRNA-210 levels in patients with hereditary hemorrhagic telangiectasia and pulmonary arteriovenous malformations: a potential new biomarker. *Biomarkers*, 18(1), 23-29.
doi:10.3109/1354750X.2012.728624
- Zheng, H., Zhang, L., Zhao, Y., Yang, D., Song, F., Wen, Y., Hao, Q., Hu, Z., Zhang, W., & Chen, K. (2013). Plasma miRNAs as Diagnostic and Prognostic Biomarkers for Ovarian Cancer. *PLoS One*, 8(11), e77853. doi:10.1371/journal.pone.0077853
- Zhou, J., Gong, G., Tan, H., Dai, F., Zhu, X., Chen, Y., Wang, J., Liu, Y., Chen, P., Wu, X., Wen, J. (2015). Urinary microRNA-30a-5p is a potential biomarker for ovarian serous adenocarcinoma. *Oncology Reports*, 33.6, 9.

Appendix A: Real time PCR Amplification Plot



Appendix A Figure: Real-time PCR amplification plot for the serum and tissue samples. The real-time PCR experiment was performed to quantify the levels of miR-590-3p, as well as the spike-in control Cel_miR-39-3P miRNA mimic in the serum samples and the endogenous control U6 snRNA in the tissue samples. The amplification plot displays the change of fluorescence (y-axis) during PCR cycling (x-axis). Individual curves are grouped into similar quantified concentrations by color.

**Appendix B: Quantitative Real-Time RT-PCR
Comparative C_T Analysis
Serum Samples**

Average Normal Serum Normalized Ct value=	33.8
Median Spike-In control Ct value =	24.235

Sample	MiR-590-3p Avg. C _T	Std. Dev.	Spike-In control Avg. C _T	Std. Dev.	Normalization Factor	Median normalized ΔC _T (miR-590-3p + Normalization factor)	Std. Dev.	ΔΔC _T = (ΔCT Cancer -average ΔCT normal)	Std. Dev.	MiR-590-3p Relative to Avg. Normal (2 ^{-ΔΔC_T})	Fold Change Relative to Normal	Log ₁₀ (2 ^{-ΔΔC_T})
NS1	35.75		24.09									
	34.6		23.69									
	35.18	0.81	23.89	0.28	0.34	35.52	0.86	1.72	0.86	0.30	-3.30	-0.52
NS2	33.15		20.4									
	32.52		20.66									
	32.84	0.45	20.53	0.18	3.71	36.54	0.48	2.74	0.48	0.15	-6.69	-0.83
NS3	30.49		23.19									
	30.54		22.94									
	30.52	0.04	23.07	0.18	1.17	31.69	0.18	-2.11	0.18	4.32	4.32	0.64
NS4	33.56		25.11									
	33.39		24.76									
	33.48	0.12	24.94	0.25	-0.70	32.78	0.28	-1.02	0.28	2.03	2.03	0.31

NS5	33.73		23.2										
	33.87		23.05										
	33.80	0.10	23.13	0.11	1.11	34.91	0.15	1.11	0.15	0.46	-2.16	-0.34	

NS6	34.39		24.44										
	33.41		24.72										
	33.90	0.69	24.58	0.20	-0.34	33.56	0.72	-0.24	0.72	1.18	1.18	0.07	

BS1	32.86		25.31										
	32.22		25.05										
	32.54	0.45	25.18	0.18	-0.95	31.60	0.49	-2.20	0.49	4.60	4.60	0.66	

CS1	32		24.36										
	32.54		24.01										
	32.27	0.38	24.19	0.25	0.05	32.32	0.46	-1.48	0.46	2.78	2.78	0.44	

CS2	27.53		21.99										
	26.84		21.05										
	27.19	0.49	21.52	0.66	2.72	29.90	0.82	-3.90	0.82	14.90	14.90	1.17	

CS9	24.3		22.92										
	24.78		22.45										
	24.54	0.34	22.69	0.33	1.55	26.09	0.48	-7.71	0.48	208.97	208.97	2.32	

CS10	19.87		21.36										
	20.52		21.37										
	20.20	0.46	21.37	0.01	2.87	23.07	0.46	-10.73	0.46	1700.97	1700.97	3.23	

CS11	30.4		23.06										
	29.72		21.18										
	30.06	0.48	22.12	1.33	2.12	32.18	1.41	-1.62	1.41	3.08	3.08	0.49	

CS12	28.86		25.52									
	29.28		25									
	29.07	0.30	25.26	0.37	-1.03	28.05	0.47	-5.75	0.47	53.90	53.90	1.73

CS13	34.37		26.23									
	34.82		25.87									
	34.60	0.32	26.05	0.25	-1.82	32.78	0.41	-1.02	0.41	2.02	2.02	0.31

CS14	33.11		25.08									
	32.93		24.99									
	33.02	0.13	25.04	0.06	-0.80	32.22	0.14	-1.58	0.14	2.98	2.98	0.47

CS15	23.39		25.98									
	24.2		25.76									
	23.80	0.57	25.87	0.16	-1.64	22.16	0.59	-11.64	0.59	3185.14	70.00	3.50

CS16	29.83		32									
	29.9		33.67									
	29.87	0.05	32.84	1.18	-8.60	21.27	1.18	-12.53	1.18	5923.13	5923.13	3.77

CS17	29.55		29.9									
	32.36		29.9									
	30.96	1.99	29.90	0.00	-5.67	25.29	1.99	-8.51	1.99	363.84	363.84	2.56

CS18	34.92		19.02									
	32.69		19.69									
	33.81	1.58	19.36	0.47	4.88	38.69	1.65	4.89	1.65	0.03	-29.61	-1.47

CS19	31.37		20.21									
	31.86		18.91									
	31.62	0.35	19.56	0.92	4.68	36.29	0.98	2.49	0.98	0.18	-5.63	-0.75

**Appendix C: Quantitative Real-Time RT-PCR
Comparative C_T Analysis
Tissue samples**

Average Normal Normalized Ct value = 9.11

Sample	MiR-590-3p Avg. CT	Std. Dev.	U6 snRNA Avg. CT	Std. Dev.	ΔC_T (MiR-590-3p – U6snRNA)	Std. Dev.	$\Delta\Delta C_T =$ (ΔC_T Cancer – average ΔC_T normal)	Std. Dev.	MiR-590-3p Relative to Avg. Normal ($2^{-\Delta\Delta C_T}$)	Fold Change Relative to Normal	$\text{Log}_{10}(2^{-\Delta\Delta C_T})$
N1	31.81		21.65								
	31.89		22.53								
	29.93		20.9								
	29.08		20.82								
	30.68	1.40	21.48	0.80	9.20	1.61	0.09	1.61	0.9403	-1.06	-0.03
N2	30.59		21.84								
	29.19		21.33								
	29.89	0.99	21.59	0.36	8.31	1.05	-0.81	1.05	1.7517	1.75	0.24
N3	30.69		21.17								
	29.22		20.69								
	29.96	1.04	20.93	0.34	9.03	1.09	-0.09	1.09	1.0634	1.06	0.03
N4	29.49		15.61								
	29.83		18.21								
	29.66	0.24	16.91	1.84	12.75	1.85	3.64	1.85	0.0804	-12.43	-1.09

N5	28.58		19.26								
	28.51		19.26								
	28.55	0.05	19.26	0.00	9.29	0.05	0.17	0.05	0.8881	-1.13	-0.05

N6	24.93		18.62								
	25.15		16.37								
	25.04	0.16	17.50	1.59	7.55	1.60	-1.57	1.60	2.9665	2.97	0.47

B1	26.12		17.19								
	26.06		17.52								
	26.09	0.04	17.36	0.23	8.74	0.24	-0.38	0.24	1.3002	1.30	0.11

C1	32.68		24.73								
	35.02		20.23								
	29.76		20.92								
	29.38		20.55								
	33.85	1.65	22.48	3.18	11.37	3.59	2.26	3.59	0.2093	-4.78	-0.68

C2	31.5		24.7								
	29.65		27.5								
	30.58	1.31	26.10	1.98	4.48	2.37	-4.64	2.37	24.9117	24.91	1.40

C3	34.92		21.58								
	33.9		21.12								
	34.41	0.72	21.35	0.33	13.06	0.79	3.95	0.79	0.0649	-15.41	-1.19

C4	29.22		22.39								
	29.85		22.47								
	29.54	0.45	22.43	0.06	7.11	0.45	-2.01	0.45	4.0243	4.02	0.60

C5	32.42		21.14								
	30.28		22.96								

	31.35	1.51	22.05	1.29	9.30	1.99	0.19	1.99	0.8789	-1.14	-0.06
--	--------------	------	--------------	------	------	------	------	------	--------	-------	-------

C6	29.8		21.2								
	28.87		21.67								
	29.34	0.66	21.44	0.33	7.90	0.74	-1.21	0.74	2.3194	2.32	0.37

C7	25.75		18.09								
	25.69		18.63								
	25.72	0.04	18.36	0.38	7.36	0.38	-1.75	0.38	3.3723	3.37	0.53

C8	24.62		20.13								
	24.87		20.89								
	24.75	0.18	20.51	0.54	4.24	0.57	-4.88	0.57	29.4205	29.42	1.47

C9	27.78		21.02								
	28.3		21								
	28.04	0.37	21.01	0.01	7.03	0.37	-2.08	0.37	4.2391	4.24	0.63

C10	24.69		18.87								
	24.81		18.5								
	24.75	0.08	18.69	0.26	6.07	0.28	-3.05	0.28	8.2749	8.27	0.92

C11	26.71		20.92								
	26.91		21.47								
	26.81	0.14	21.20	0.39	5.62	0.41	-3.50	0.41	11.3039	11.30	1.05

C12	26.82		19.87								
	26.68		19.49								
	26.75	0.10	19.68	0.27	7.07	0.29	-2.04	0.29	4.1232	4.12	0.62

C13	27.15		22.41								
------------	-------	--	-------	--	--	--	--	--	--	--	--

	27.26		21.34								
	27.21	0.08	21.88	0.76	5.33	0.76	-3.78	0.76	13.7728	13.77	1.14

C14	29.01		19.45								
	30.75		19.45								
	29.88	1.23	19.45	0.00	10.43	1.23	1.32	1.23	0.4016	-2.49	-0.40

C15	25.43		19.87								
	25.41		19.73								
	25.42	0.01	19.80	0.10	5.62	0.10	-3.49	0.10	11.2648	11.26	1.05

C16	28.7		21.71								
	28.71		21.97								
	28.71	0.01	21.84	0.18	6.87	0.18	-2.25	0.18	4.7527	4.75	0.68

C17	26.9		18.56								
	25.87		18.06								
	26.39	0.73	18.31	0.35	8.08	0.81	-1.04	0.81	2.0544	2.05	0.31

C18	24.43		18.42								
	25.52		18.35								
	24.98	0.77	18.39	0.05	6.59	0.77	-2.52	0.77	5.7507	5.75	0.76

C19	23.18		16.41								
	22.92		17.01								
	23.05	0.18	16.71	0.42	6.34	0.46	-2.77	0.46	6.8388	6.84	0.83

C20	28.11		18.62								
	27.26		18.74								
	27.69	0.60	18.68	0.08	9.01	0.61	-0.11	0.61	1.0783	1.08	0.03

Appendix D: IRB Approval

CASE #2013-2014-093



To: Heba Shawer
Cc: Hind El Helaly
From: Atta Gebril, Chair of the IRB
Date: Feb 28, 2014
Re: Approval of study

This is to inform you that I reviewed your revised research proposal entitled "The expression pattern of miRNA-590-3P in epithelial ovarian cancer is a potential diagnostic biomarker for ovarian cancer early diagnosis," and determined that it required consultation with the IRB under the "expedited" heading. As you are aware, the members of the IRB suggested certain revisions to the original proposal, but your new version addresses these concerns successfully. The revised proposal used appropriate procedures to minimize risks to human subjects and that adequate provision was made for confidentiality and data anonymity of participants in any published record. I believe you will also make adequate provision for obtaining informed consent of the participants.

Please note that IRB approval does not automatically ensure approval by CAPMAS, an Egyptian government agency responsible for approving some types of off-campus research. CAPMAS issues are handled at AUC by the office of the University Counsellor, Dr. Amr Salama. The IRB is not in a position to offer any opinion on CAPMAS issues, and takes no responsibility for obtaining CAPMAS approval.

This approval is valid for only one year. In case you have not finished data collection within a year, you need to apply for an extension.

Thank you and good luck.

A handwritten signature in black ink that reads "Atta Gebril".

Dr. Atta Gebril
IRB chair, The American University in Cairo
2046 HUSS Building
T: 02-26151919
Email: agebril@aucegypt.edu

Appendix E: Patient's Consent Forms



Documentation of Informed Consent for Participation in Research Study

Project Title: The expression pattern of miRNA-590-3P in epithelial ovarian cancer is a potential diagnostic biomarker for ovarian cancer early diagnosis.

Principal Investigator: Heba Shawer.

Biotechnology Program, American University in Cairo, New Cairo, 11835 Egypt

E-mail: Hebashawer@aucegypt.edu.

*You are being asked to participate in a research study.

The purpose of the research is to study the expression of certain molecule in ovarian cancer tissue samples. The Successful completion of this project could provide better explanation to the genetic background of the disease, and the potential gene therapies.

The findings of the study may be published and/or presented in conferences.

The expected duration of the study is one year. On completion of the thesis, the data will be retained for a further six months, and then destroyed.

*The procedures of the research will be as follows: The level of certain molecule will be analyzed in ovarian cancer tissues and in the patient's blood samples using real time polymerase chain reaction (RT-PCR) method. This molecule in the patients' serum will be examined to evaluate the possibility to be used as a biomarker and whether it can give indication for the tumor stages.

*There *will not be* any risks or discomforts associated with this research. As, nothing will be taken for research purpose only. The specimens will not be collected specifically for the research project. We will only use portion of the samples that are collected for medical purpose.

*There *will not be* benefits to you from this research. However, you will make a chief contribution to develop the information known about ovarian cancer.

*The information you provide for purposes of this research *is* anonymous. This information will be kept in a password-protected personal laptop. Only the principle investigator of the study, the thesis advisor and the surgeon providing us with the samples will have access to the research data. No clues to your identity appear in the thesis; your identity in the thesis or any research paper will be entirely anonymous.

Questions about the research, my rights, or research-related injuries should be directed to Heba Shawer.

*Participation in this study is voluntary. Refusal to participate will involve no penalty or loss of benefits to which you are otherwise entitled. You may discontinue participation at any time without penalty or the loss of benefits to which you are otherwise entitled.

Signature _____

Printed Name _____

Date _____

استمارة موافقة مسبقة للمشاركة في دراسة بحثية

عنوان البحث : دراسة امكانية استخدام مركب في سرطان المبيض الظاهري في التشخيص المبكر لسرطان المبيض.

الباحث الرئيسي: هبة محمود شاور. طالبة ماجستير بالجامعة الامريكية بالقاهرة.
البريد الالكتروني: hebashawer@aucegypt.edu
الهاتف: ٠١٠٠١٧٣٩٤٠٩

انت مدعو للمشاركة في دراسة بحثية عن وجود مركب معين في سرطان المبيض و امكانيه استخدامه في التشخيص المبكر لسرطان المبيض. النجاح في الانتهاء من هذا المشروع قد يوفر تفسيراً افضل للخلفية الجينية للمرض و العلاجات الجينية المحتمله.

هدف الدراسة هو الوصول لوسيلة جديدة للتشخيص المبكر لسرطان المبيض.

نتائج البحث ستنتشر في دوريه متخصصه أو مؤتمر علمي أو ربما كليهما.

المدة المتوقعة للمشاركة في هذا البحث هي سنة واحده. بعد الانتهاء من الدراسة، سوف يتم الاحتفاظ بالبيانات لمدة ستة اشهر اخري ثم التخلص منها.

اجراءات الدراسة تشتمل علي دراسة جزء من الورم الذي استاصله الجراح لاسباب طبية. سوف تكون هوية المريض مجهولة في الدراسة أو اي مؤتمر علمي.

لا يوجد مخاطر متوقعة من المشاركة في هذه الدراسة. وذلك لان العينات لن تؤخذ خصيصاً من اجل الدراسة البحثية. سوف نستخدم فقد جزء من العينات التي تم اخذها لاجراض طبية.

الاستفادة المتوقعة من المشاركة في البحث: قد لا توجد استفادة شخصية من البحث. و لكنه سوف يسهم في زيادة المعرفة المعلوماتية عن سرطان المبيض.

السرية واحترام الخصوصية: المعلومات التي ستدلى بها في هذا البحث سوف تكون فيها هويتك غير محددة . و سوف تحفظ هذه المعلومات في جهاز كمبيوتر محمي بكلمة مرور سرية و لن يطلع عليها سوي الباحث الرئيسي و المشرف علي البحث و الجراح الذي يزودنا بالعينات. ستكون هويتك غير محددة في اي دوريه متخصصه أو اي مؤتمر علمي خاص بالبحث.

أي أسئلة متعلقة بهذه الدراسة أو حقوق المشاركين فيها أو عند حدوث أي اصابات ناتجة عن هذه المشاركة يجب ان توجه الي هبة محمود شاور.

ان المشاركة فى هذه الدراسة ماهى الا عمل تطوعى, حيث أن الامتناع عن المشاركة لايتضمن أى عقوبات أو فقدان أى مزايا تحقق لك. ويمكنك أيضا التوقف عن المشاركة فى أى وقت من دون عقوبة أو فقدان لهذه المزايا.

الامضاء:

اسم المشارك :

التاريخ :/...../.....

Appendix F: Copyrights Form

Heba Shower
American University in Cairo,
Biotechnology master's program
AUC Avenue, P.O. Box 74.
New Cairo 11835, Egypt.

Date:

Dear Heba:

I, Aya El Sewi hereby authorize Heba Shower to include my data related
to Semiquantitative in her Master thesis.
PCR

Sincerely,

